BAW-3376-1
AEC R&D Report
TID-4500, 35th Ed.
UC-80

IRRADIATION PERFORMANCE OF THORIA-URANIA FUEL MATERIALS

Quarterly Technical Report No. 1

May - September 1964

Approved by B. W. Whitaker
Program Manager

C. R. Johnson
Technical Manager

Submitted to
THE UNITED STATES ATOMIC ENERGY COMMISSION
by
THE BABCOCK & WILCOX COMPANY
Nuclear Development Center
Lynchburg, Virginia

DISCLAIMER

THIS PAGE
WAS INTENTIONALLY
LEFT BLANK

ABSTRACT

This report describes the work accomplished during the period May 1 to September 30, 1964, on the Irradiation Performance of Thoria-Urania Fuel Materials. The objectives of the program are as follows:

1. To establish, experimentally, physical properties of thoria-urania that are of interest to the reactor designer.
2. To present the physical property data in a form suitable for engineering application.

The thermal conductivity and gas retention and release characteristics of sol-gel thoria-urania fuel will be emphasized. Pelletized fuel will be examined to standardize the experimental equipment and to provide data for correlation with available information.

The major effort during this report period involved preparation of the work program and planning and design of the experiments. Applicable information from similar programs was examined through literature searches and visits. Objectives of all tasks were analyzed to ensure compatibility with the over-all program objective. Design of experiments for all tasks was started, and some equipment and supplies were procured.

THIS PAGE
WAS INTENTIONALLY
LEFT BLANK

CONTENTS

CONTENTS (Cont'd)

List of Tables

List of Figures

1. INTRODUCTION

Complete exploitation of the advantages of thorium as a fertile material in thermal and particular resonant spectrum reactors has been inhibited by the lack of quantitative physical property data for thoria and thoria-urania fuels. Thoria and thoria-urania solid solutions have not been investigated to the extent of pure urania. The meager information available has been deduced from extrapolation of urania data to thoria data or produced from the few isolated programs dealing with thoria itself. No reliable performance information on thoria-urania fuel is available, especially in the higher performance areas, and there is no knowledge of the materials ultimate performance limits.

This contract provides for a series of experiments directed toward establishing certain physical properties of thoria-urania fuel materials that are necessary for improved reactor core design. Gas content and gas release characteristics of thoria-urania fuel produced by the sol-gel method will be investigated to provide the core designer with insight into internal gas pressures to be expected during operation of this fuel under varying power conditions. Thermal conductivity during nuclear self-heating will be studied at power levels sufficient to raise central fuel temperatures to the melting point. The thermal conductivity experiments will be performed on sol-gel-produced powdered fuel and on pelletized thoria-urania to establish a degree of correlation to similar work carried out on urania pellets and to compare directly the performance capabilities of pellets and powdered fuel. The thermal conductivity data will enable the core designer to calculate internal fuel temperatures and temperature gradients under varying power conditions so that he can design better fuel elements and predict thermal capabilities and core life more accurately.

The program is divided into six experimental tasks and an additional task providing supervision, reports, and technical support. The experimental tasks are as follows:

Task No.	Supporting Measurements
02	Gas Permeability of Irradiated Fuel
03	Sorbed Gas Release Determinations
	Thermal Conductivity
04	Unirradiated Fuel Thermal Conductivity
05	Irradiated Fuel Thermal Conductivity
	Gas Release
06	Dynamic Inpile Fission Gas Release Experiment
07	Static Gas Release Experiment

2. GAS PERMEABILITY OF IRRADIATED FUEL — TASK 02
(G. C. Robinson, Task Leader; A. C. Batten)

2.1. Task Objective

The objective of this task is to obtain information on the gas permeability characteristics of unirradiated and irradiated specimens of thoria-urania at both room and elevated temperatures. Permeability of structurally altered fuel to fission gas will be examined by testing specimens from the unirradiated fuel thermal conductivity experiments (Task 04). Irradiated specimens from the fission gas release experiments (Tasks 06 and 07) will also be tested.

2.2. Task Description

Fuel rods are normally designed to contain some void volume to allow accumulation of gases released from the fuel. The rate at which locally released gases permeate to expansion voids is of interest in predicting gas movement and pressure buildup within fuel rods. In fission gas analysis of irradiated fuel specimens, accuracy depends on the complete removal of all the gases within the open pores of the fuel. Fission gases have been observed to emanate from fuel specimens long after the analysis has been completed, indicating that not all of the gas was initially released to the sampling system.

During core operation it is anticipated that thermal excursions will cause variations in fission gas pressures, resulting in large variations of driving force for movement of the gas through the structure. The local pressure buildup due to a pulse of fission gases released to open porosity depends on the capability of the fuel to dissipate these gases.

The initial program effort is directed toward the design and construction of an apparatus capable of testing the gas permeability of thoria-urania fuel specimens. Unirradiated fuel rod specimens will

contain as-fabricated structures as well as altered structures simulating those of inpile exposure. Irradiated specimens will be obtained from other tasks of this program.

Since both pellet-type and vibratory compacted fuel will be investigated, and since little permeability information on nuclear fuels has been reported, it is necessary to determine the magnitude of the variables involved so that a suitable apparatus for making the permeability measurements can be designed. This will be accomplished by preliminary bench-type tests on both pellet and vibratory compacted fuel. The information obtained from these preliminary tests will then be used to design an apparatus capable of making precision measurements for permeability calculations.

2.3. Work Accomplished During This Report Period

2.3.1. Summary

1. A literature survey of gas permeability studies was completed.
2. Bench test designs for low and high pressure measurements have been completed.
3. Materials and equipment for these bench tests have been ordered.
4. A method for sealing pellet and vibratory compacted fuel specimens has been determined.

2.3.2. Literature Survey

To determine definitive experiment requirements, a literature survey of gas permeability studies was made. The purpose of the study was to obtain information on permeability measuring devices, as well as to survey the theoretical gas flow considerations applicable to porous media. Results of the survey with a discussion and bibliography appear in Appendix A.

Permeability is defined as a measure of the capacity of a medium to transmit fluids, and is generally expressed as a coefficient having the dimensions cm^2/sec. For flow of gas through a porous medium, the permeability coefficient K is calculated from the relationship

$$K = \frac{\text{(flow rate)}}{(\Delta \text{ pressure})\ (\text{area/length})}$$

where all the factors are experimentally measured. K may result from a combination of both viscous and Knudsen gas flows within the same porous specimen, and therefore may be expressed in terms of both viscous and Knudsen flows. The expression and method of determining the specific permeability coefficients for each type of flow are given in Appendix A, which also includes information on flow and pressure measurements.

It is significant that the reported experiments were carried out at mean pressures of a few atmospheres. Postulated conditions within the fuel rod make it desirable to also determine gas flow for pressures as high as several hundred atmospheres. However, as the flow rate is increased, viscous flow may change to turbulent flow. This change may be experimentally determined from the permeability curve where deviation from a straight line occurs when turbulence is reached.

2.3.3. Bench Test Design

Since fuel pellets are pressed and sintered, the resultant structure contains less open porosity than is found in vibratory compacted fuel. As a result, it is anticipated that the permeability of these fuel types will differ greatly. It is necessary to establish a range of expected gas flow through both fuel types so that the proper measuring devices can be provided on the final permeability apparatus. It is also necessary to establish a relationship between low and high pressure flow measurements so that the need for a more complex apparatus may be determined. Simplified tests referred to as bench tests will be used to obtain information necessary for designing the final permeability apparatus.

For low pressure tests where the flow is expected to be low, flow will be measured by determining the pressure rise in a known volume that has been previously evacuated. Such a method is very sensitive to low flow rates. This bench test will use an apparatus having a vacuum pump connected to 5000 cc volumes on each side of the specimen. Gas at a constant pressure will be fed to one side of the specimen, and the pressure rise on the other side will be measured with

an absolute pressure indicator having a range of 0-800 mm Hg. By having known volumes on both sides of the specimen, dynamic pumping and pressure decay tests can also be made readily on the same specimens.

For high pressure tests it is more economical to have a simple system capable of withstanding pressures up to 2500 psi. Gas will be fed directly to one side of the specimen, and the flow on the opposite side will be measured by volume displacement. The downstream pressure will be controlled by a regulating valve, and pressures on both sides of the specimen will be measured with test gauges.

Necessary material and equipment for the bench tests have been ordered.

2.3.4. Elevated Temperature Studies

Elevated temperature studies are considered necessary since data specifically defining the effect of temperature on gas permeability of fuels is lacking. Also, specimens having the altered fuel structures will contain cracks which are expected to close (and possibly heal) at elevated temperatures. It is anticipated that this would affect the permeability as compared with room temperature experiments. For these reasons, temperature is presently considered a variable in the proposed experiments.

In the bench test, elevated temperatures within the fuel will be obtained by use of electrical heater tapes wrapped around the specimen in the area of the fuel. The desired temperature will be controlled by the regulation of power to the tape as determined by thermocouples on the specimen. Sufficient time will be allowed for the fuel to reach equilibrium temperature. Because of the high-temperature strength limitations of cladding materials which have expansion coefficients less than that for the fuel, all elevated temperature measurements will be restricted to the low pressure apparatus. Analysis of the results will then determine whether elevated temperature measurements will be necessary at the high pressures.

2.3.5. Specimen Design

Vibratory compacted fuel specimens will consist of a half-inch-OD tube approximately 30 inches long having fuel located at

the center 10 inches. The fuel powder will be held in place by means of microporous stainless steel filter discs (20 micron porosity) supported by an internal sleeve extending to each end of the tube, where the sleeve and tube will be welded. The tube will be attached to the apparatus by means of bite-type pressure fittings. For vibratory compacted fuel rods, the assumption is made that the fuel powder is tightly compacted against the tube walls to effect a seal. To prevent possible relaxing of this seal as the temperature is raised, Zircaloy-2 was chosen for the specimen tubing since this material has a coefficient of expansion less than that of the fuel. At elevated temperatures the seal at the tube wall should become tighter. It is planned to run tests which will provide information on the effectiveness of the seal, but details on these tests have not been firmed up at this time. The sleeve material supporting the filter discs will also be made from Zircaloy-2 tubing, and sufficient clearance between the filter disc and the tube wall will be provided to allow for the greater expansion of the stainless steel.

Pellet-type fuel specimens will consist of a fuel pellet brazed to the wall of Zircaloy-2 tubing. Prior to brazing, the peripheral surface of the pellet will be coated with copper or other suitable metal which can be brazed. The brazed joint will provide a seal at both room and elevated temperatures since the joint will be placed into compression as the temperature is raised.

For the bench tests UO_2 fuel will be used in both pellet and powder forms since this type of fuel is immediately available.

2.4. Planned Work for Next Report Period

During the next report period, the apparatus for the bench tests will be assembled and tested for leaks. Specimens for the bench tests will be prepared, and then the test runs on these specimens will be made.

3. SORBED GAS RELEASE DETERMINATIONS — TASK 03
(C. J. Halva, Task Leader)

3.1. Task Objective

The objective of this task is the identification of gases and the determination of the quantity of absorbed and adsorbed gases released from unirradiated sol-gel fuel as a function of temperature.

3.2. Task Description

The quantities and types of sorbed gases in nuclear fuels vary with the type of fuel and method of production. Specific studies have been made on various types of nuclear fuels[1,2,3,4], and fuels manufactured by the sol-gel process have been evaluated in abbreviated studies at ORNL[5]. Further gas release studies are continuing at ORNL[6]. Our primary interest is the determination of sorbed gases in fuels produced by the sol-gel process at the Babcock & Wilcox Nuclear Development Center, since some of these fuels will be used for irradiation experiments in other portions of this program.

The quantity of sorbed gases released bears a direct relationship to the resultant fuel rod internal gas pressure. Allowances must be made in either the fuel rod design or by the addition of degassing steps in the production procedure to remove excessive amounts of potentially harmful gases if they are found to be present. The chemical makeup of the released gases is important in determining at what point the gases were added in the production process and in determining whether the released gases will be deleterious to the cladding material. Both of these factors influence the final design and interpretation of the associated irradiation experiments.

The objective will be accomplished by heating fuel specimens in a vacuum to preselected temperatures from 100 C to approximately 2000 C, collecting a given quantity of the evolved gas, and analyzing

it using mass spectrometer and gas chromatograph methods. Variations in release rate, quantity, and species of released gases will be determined as functions of temperature, time, fuel composition, fuel particle size, and other production variables.

3.3. Work Accomplished During This Report Period

3.3.1. Summary

The experimental approach to the determination of sorbed gases in nuclear fuels has evolved into a manyfold study of the various parameters. Two preliminary experiments to determine the quantity and the species of gas released as a function of time and temperature have been designed. These experiments are mainly vacuum extraction system checkout tests and will be used to evaluate our handling methods and procedures. The third, and major, experiment incorporating the methods developed in the first two experiments has been planned to evaluate the effects of fuel composition, particle size, and other production variables on the quantity and species of gas released. The vacuum extraction system for collecting the sorbed gases at various pressures has been designed and constructed and is in its final checkout. Fuel for this program has been scheduled for production. Analytical control methods and sampling methods have been developed. The gas analysis apparatus should be completed by the middle of the next report period.

3.3.2. Experimental Design

A system has been fabricated for the quantitative extraction and collection of the released gases from heated fuel specimens. These collected gases will then be analyzed by both gas-chromatographic and mass-spectrometric methods. The gas chromatograph will be programmed for the expected evolved gases; the results obtained from this method will be compared with those from the mass-spectrometric method. If it becomes evident as the experiments progress that the precision and accuracy of the two systems are nearly the same, quantitative mass-spectrometric identification of the gases may be stopped in favor of the faster chromatographic methods. However, qualitative identification of the collected gases and possibly other gases will be

periodically checked with the mass spectrometer. The specific experiments to be performed are outlined below.

3.3.2.1. Preliminary Determination of the Quantity of Sorbed Gases Released Vs Temperature

Purpose

This experiment is designed to determine the suitability of the extraction system for the following:

1. Determination of total gases released from a series of selected thoria and thoria-urania specimens as a function of temperature and time.
2. Observation of the rate of gas release as a function of temperature.
3. Identification and quantitative determination of the total gases evolved.

Procedure

Selected powder- and compacted-thoria-urania sol-gel fuel specimens in a vacuum system will be heated to predetermined temperatures at a given rate and held for a period of time. The pressure buildup and gas release rate will be studied during this period. The gases will be collected at the end of this experiment and quantitatively identified. The techniques developed in measuring temperature and pressure, the necessary time for pressure equilibration at a given temperature, as well as techniques for collection, transfer, and identification of released gases will be utilized in the third experiment of this series.

3.3.2.2. Preliminary Determination of the Species of Released Gases Vs Temperature

Purpose

This experiment is designed to determine the suitability of the experimental apparatus to measure:

1. The species and quantity of sorbed gas from ThO_2 and ThO_2-UO_2 sol-gel as a function of temperature and time at temperature.
2. The release rate as a function of temperature.

Procedure

Selected thoria-urania sol-gel fuel specimens will be heated at a predetermined rate to a preselected temperature and held at that temperature, after which the total quantity of sorbed gas evolved will be measured and removed from the system for quantitative identification. The temperature will then be raised to another selected setting, and the procedure will be repeated. The rate of release will be studied and observed to determine whether release "bursts" are taking place. The procedures developed here will be used in the next experiment.

3.3.2.3. Fuel Composition and Subsequent Gas Release Vs Temperature

Purpose

This experiment is designed to determine the effects of different variables in sol-gel fuel preparation on the quantity, release rate, and species of sorbed gas at different temperatures.

Procedure

The techniques developed in the preceding two experiments will be used to study the effects of varying the Th-U ratio, particle size, grinding, and other variables encountered in the preparation of sol-gel fuel specimens.

3.3.3. Progress on Sorbed Gas Studies

Progress on the sorbed gas studies program has occurred in several areas. Each of these areas is discussed individually in the following sections.

3.3.3.1. Sol-Gel Fuel Production

Thoria-urania sol-gel fuel of varying composition for use in these studies will be produced by The Babcock & Wilcox Company's Feed Materials Plant. The following runs are scheduled for production of 7 kg per run of sol-gel fuel:

Run No.	ThO_2, %	UO_2, %
1	100.00	0.00
2	98.75	1.25
3	97.50	2.50
4	96.25	3.75
5	95.00	5.00
6	92.50	7.50
7	90.00	10.00

These are approximate compositions, and an error of ±10% of the total UO_2 present will be acceptable. Accurate analytical determinations will be made on each batch. Both the uranium and the thorium in these fuels will have natural composition.

3.3.3.2. Analytical Methods

The analytical methods to determine the uranium, thorium, nitrate, and density for the sol-gel process have been developed using methods incorporated by ORNL and other laboratories. Figure 3-1 shows the general scheme of analyses for the entire sol-gel process. The analytical determinations listed are essential to understand and evaluate the entire process. The following methods of analysis for the uranium, thorium, and nitrate have the relative precisions shown.

Constituent	Method of analysis	Precision, %
U	Coulometric	0.5
	Potentiometric	0.6
Th	Volumetric via EDTA	0.5
	Colorimetric with Thoren	2.0
NO_3	Colorimetric with Indigo Carmine	5.0
	Ion Exchange	Not determined

Density will be measured using pyncnometer techniques. Moisture determinations will be based on loss of weight at 125 C in air.

All of the aforesaid techniques will be used to analyze the fuels produced for the sorbed gases program.

3.3.3.3. Sol-Gel Sampling Techniques

Samples will be collected at various locations after firing in the sol-gel process to determine the gas content of the final product. The flow sheet (Figure 3-2) indicates the points of sample collection. Bulk samples of as-produced material will be analyzed from the furnace. Since a question may be raised concerning whether the sol-gel oxide will absorb gases after firing, the furnace oxide sample will be split into two portions. One portion will be stored in air until gas analyses are made; the other will be stored in an inert atmosphere.

A portion of the as-purchased bulk material will be sieved into various fractions—6-16 mesh, 16-200 mesh, -200 mesh, and other sizes—to correlate the gas content of the sample with sieve size. Again samples will be stored in air and inert atmosphere to ascertain relative gas pickup tendencies.

Since some sol-gel oxide may be ground in the production process, a portion of the bulk sol-gel oxide will be ground, probably in a ball mill, to determine whether the total gas release is greater from the ground material than from the bulk material. The ground material can cause an increase in total gas content by two methods: release of entrapped gases and/or pickup of atmospheric gases due to the fine nature of the ground material. If a significant increase in gas released is noted, it will be necessary to grind the sol-gel oxide in selected atmospheres to determine how the "excess" gas is being introduced.

Samples of compacted sol-gel fuel will also be evaluated. The compacted fuel will be compared with fuels prepared by other means. These fuels will be analyzed for their gas content.

3.3.3.4. Vacuum Extraction System

The vacuum extraction system for this program has been constructed. Several vacuum collection systems were considered for the measurement of the total gases released and for the isolation and collection of these gases for quantitative determinations. Basically, the system consists of a source for heating the sample, a calibrated volume for measuring the total gases with an appropriate

pressure-measuring device, a device for concentrating the gases, and a sample collection and take-off system. The completed system design is shown schematically in Figure 3-3. A photograph of the completed vacuum system is shown in Figure 3-4.

Resistance and induction heating methods were considered. Induction heating was chosen on the basis of equipment availability, simplicity, and high temperature capability. The power supply is rated at 23.5 kva, which is more than adequate to meet the experimental requirements.

The apparatus for gas collection consists of a dosing stopcock, a McLeod gauge, and three calibrated volumes. The small volume is bounded by Stopcocks C, D, and F and includes the McLeod gauge (Figure 3-3). The intermediate volume consists of the small volume plus Sample Chamber No. 1, which is a 125 cc gas collection tube. The large volume consists of the total glass system, including the Toepler pump, McLeod gauge, induction heating chamber, and Chambers No. 1 and No. 2. The volumes of the three described systems are 36.6 cc in the small volume, 174 cc in the intermediate volume, and 396 cc in the large volume at STP. Since the maximum pressure measuring capability of the McLeod gauge is 5 mm of Hg, 5 gm fuel samples that contain between 0.009 and 0.5 cc/gm can be accommodated.

Several systems were available for concentrating the gas sample either to determine its volume or to collect it for gas analysis. Liquid air freeze-down tubes, absorption devices, mercury diffusion pumps, and Toepler pumps were considered as possible concentrating units. The expected presence of oxygen in the sorbed gases eliminated freeze-down tubes since either liquid oxygen or helium would have to be used. Absorption devices such as a titanium sponge or activated charcoal were deemed unusable since some of the expected gases in the fuel could not be readily removed from these agents.

Either a mercury diffusion pump or a Toepler pump would be suitable for concentrating the gases. The Toepler pump was selected because of its convenience and automatic features.

The sample collection and take-off portion of the system was designed to provide for appropriate connection to both

the gas chromatograph and mass spectrometer analysis apparatus. Regular glass collecting tubes are used for this purpose.

The primary vacuum is provided by two vacuum pumps. A Fisher portable vacuum system is used to operate the Toepler pump. This system has an ultimate vacuum of 50 microns Hg. A Welch Duo-Seal vacuum pump provides the vacuum for the rest of the system. This has an ultimate vacuum rating of less than 1 micron Hg. Ultimate pump-down readings of 5 microns Hg or less are provided by these two systems.

The sample-heating chamber consists of a 57 mm diameter Vycor tube sealed at both ends with an O-ring into a water-cooled aluminum jacket. This jacket is to prevent radiating and conducting heat from softening and/or expanding the Vycor tube at higher temperatures. An induction coil fits around this tube. The tungsten crucible containing the fuel sample is positioned on another Vycor tube having a fused silica top. A platinum-rhodium thermocouple fits into the top of the crucible. Crucibles made of carbon and molybdenum were tried, but severe degassing occurred. Vapor deposition of tungsten on the Vycor heating chamber has been observed. Different crucible materials and sealing either the present tungsten crucible or a carbon crucible with Vycor, fused silica or alumina, or some other inert, high temperature ceramic have been considered as possible methods of eliminating this problem.

3.3.3.5. Gas Analysis Apparatus

Gas samples will be analyzed using both mass spectrometric and gas chromatographic methods. The gas chromatograph to be used is a Barber-Colman Series 5000 Selecta System. This system will be initially programmed to analyze the following gases: CO, CO_2, O_2, N_2, Ar, CH_4, H_2, and water vapor. The unit has subambient temperature programming to separate Ar from O_2. Figure 3-5 is a photograph of this system.

The mass analyses will be performed on a mass spectrometer similar to the Consolidated Electrodynamics Corporation's Type 21-703 spectrometer. The spectrometer tube, magnet, source, and collector units were all built by Consolidated to Type 21-703 specifications.

The mass spectrometer is a first-order angular focusing instrument with a 60° sector magnetic field on a 12-inch radius. The instrument is composed of two major assemblies. One contains the electric controls and the readout and recording system. The other houses the vacuum system, analyzer tube, and electromagnet. Figure 3-6 is a photograph of this unit as used for solids analysis.

The gas source is being fabricated. It consists of an emission regulator, a gas inlet system with a mercury diffusion pump, and necessary modifications to allow the gas inlet to be physically installed on the present mass spectrometer.

3.4. Planned Work for Next Report Period

The gas source for the mass spectrometer and the gas chromatograph will be completed and calibrated during the next report period. The vacuum extraction system will be further calibrated, and test specimens will be degassed. Some production fuel will be evacuated, and gas samples will be analyzed for both quantity and specie. Final apparatus adjustments are expected to be accomplished.

Figure 3-1. Sol-Gel Process Control Assays

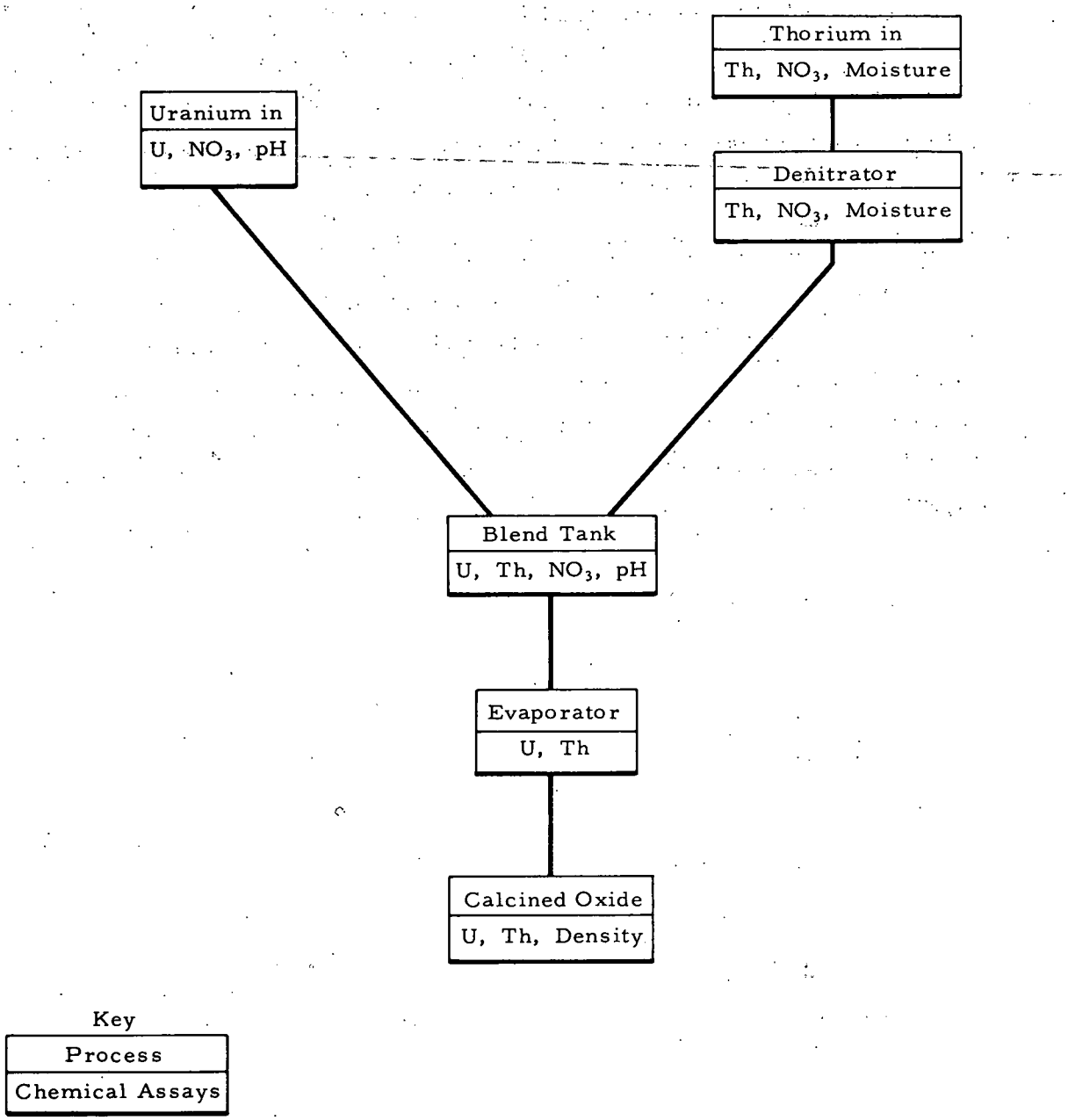

Figure 3-2. Sol-Gel Sampling Locations

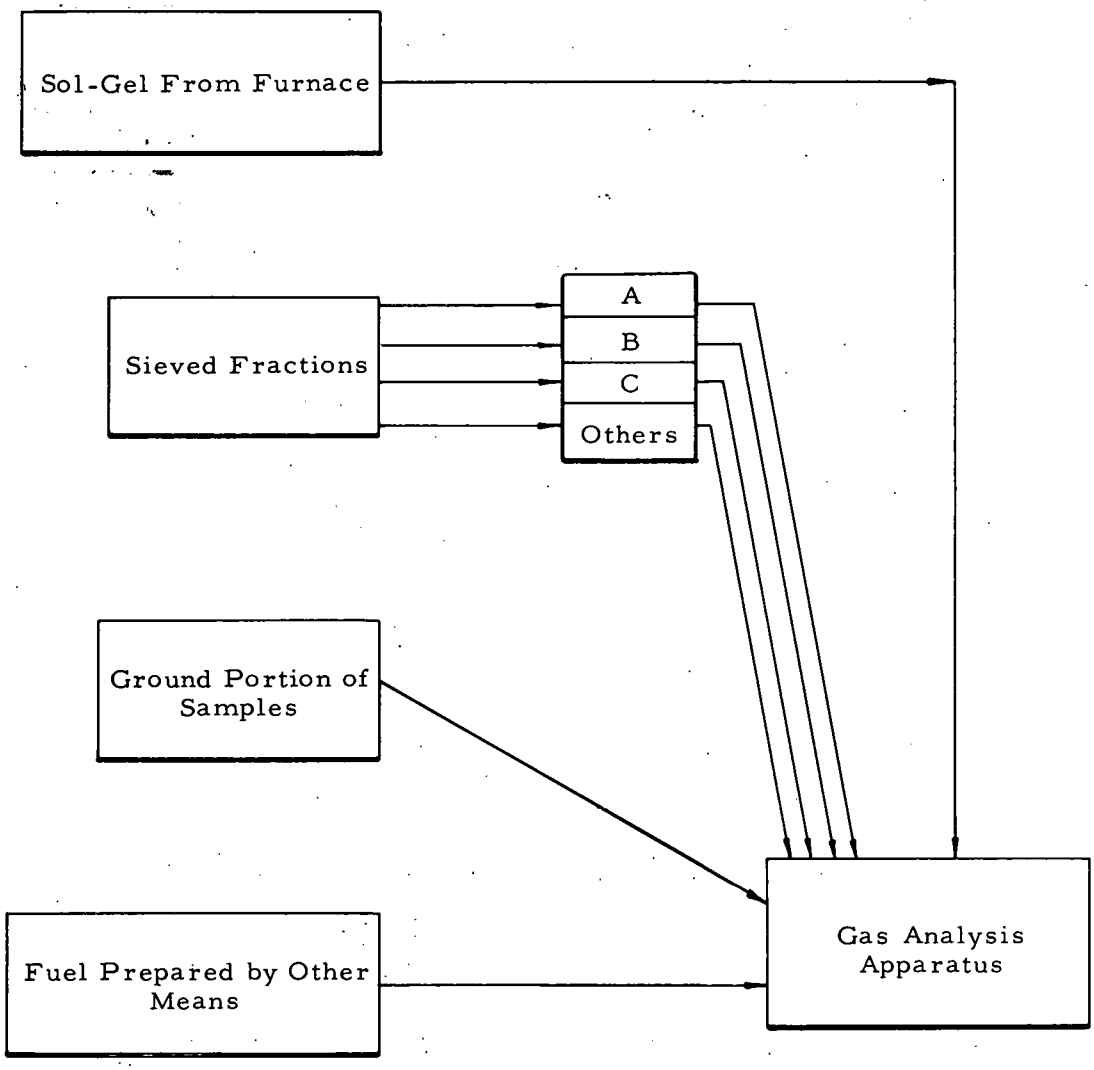

Figure 3-3. Vacuum Extraction System

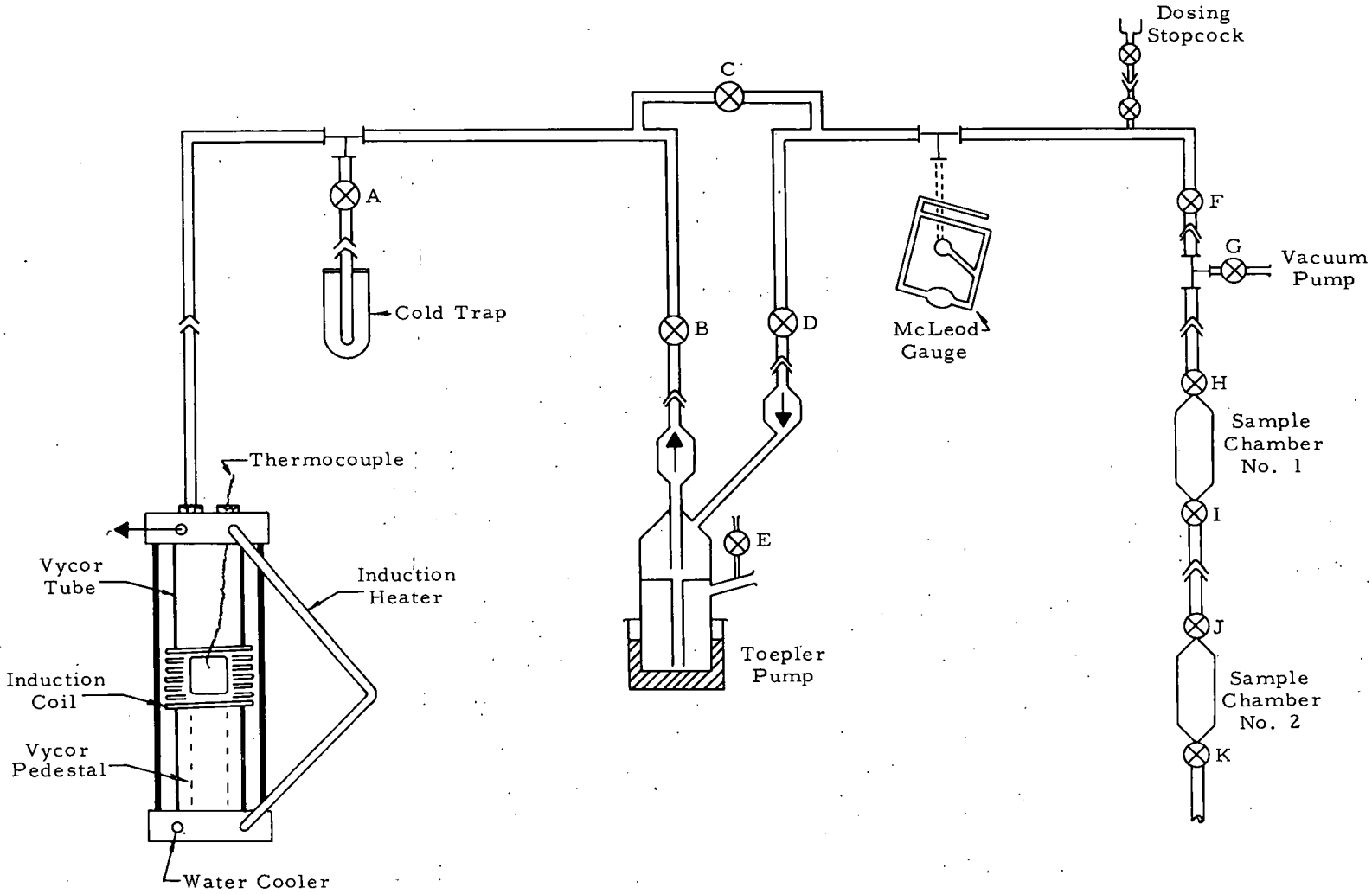

Figure 3-4. Vacuum Extraction System Photograph

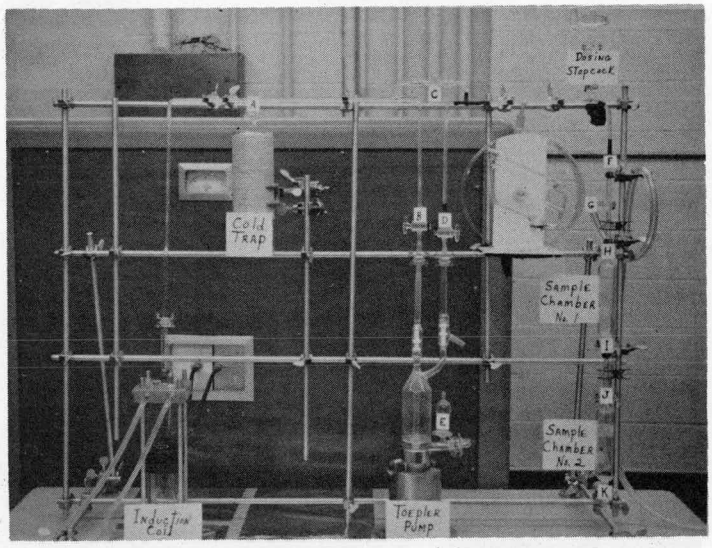

Figure 3-5. Barber-Colman Gas Chromatograph

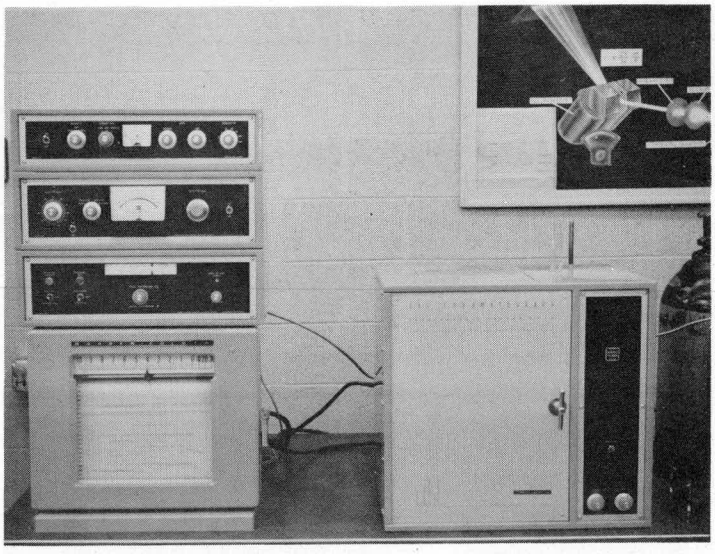

Figure 3-6. CEC Equivalent Mass Spectrometer

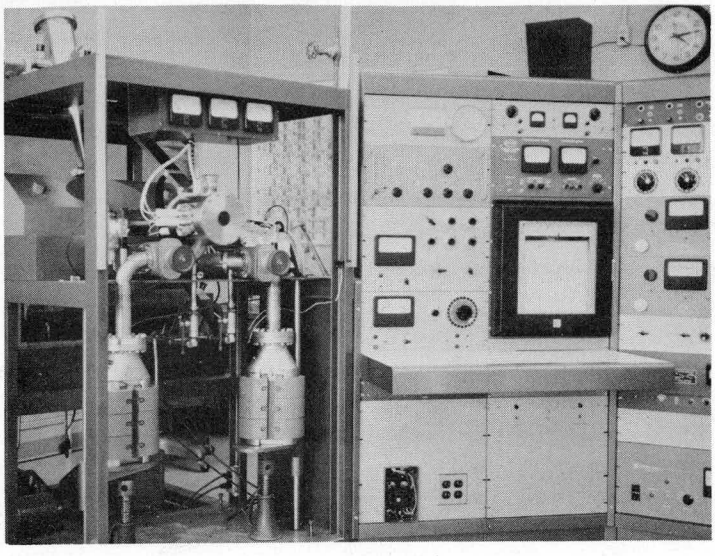

4. UNIRRADIATED FUEL THERMAL CONDUCTIVITY — TASK 04

(G. C. Robinson, Task Leader; J. M. Kerr; E. N. Harbinson)

4.1. Task Objective

The primary objective of this task is to establish a correlation between fuel structure and temperature of thoria-urania. This correlation will be used in estimating the operating temperatures of the fuel in the irradiated specimens of Tasks 05, 06, and 07. The secondary objective is the determination of the thermal conductivity of unirradiated thoria-urania to about 2500 C. These data are expected to provide a useful comparison with the inreactor thermal conductivity obtained in Task 05.

4.2. Task Description

In Task 05, the inreactor thermal conductivity of ThO_2-UO_2 will be determined from the

$$\int_{\theta_1}^{\theta_2} k d\theta$$

relationship. Since the limits of the integral must be obtained from the experiment, a method of determining the operating temperatures in the fuel is required. Customarily, these temperatures are estimated from the altered fuel structure since relationships exist between the structure components (temperature markers) and temperature. In this task, correlations between specific structure components and the temperatures required to produce the structures will be established. In order to apply these correlations to fuel structures produced in the reactor, it will be assumed that the relationship between fuel structure and temperature is not significantly altered by the reactor environment. This assumption is consistent with previous experiments of similar nature.[7]

Prior analysis of available thermal conductivity data for UO_2 and ThO_2-UO_2 indicates the need for a temperature marker in the range of 1200 C to melting in order to construct an accurate thermal conductivity relationship at temperatures up to the melting point of the fuel. The structure component or marker selected for temperature correlation must have a predictable occurrence in the temperature region of interest and must be producible in outpile experiments, where correlation with temperature will be accomplished. In this regard, the radius of initiation of columnar grain growth and equiaxed grain growth would appear to provide acceptable temperature markers for ThO_2-UO_2 because (1) the growth of columnar and equiaxed grains has been observed in both ThO_2-UO_2 and UO_2 irradiations, (2) columnar grain growth and equiaxed grain growth have been used successfully as temperature markers for UO_2 in the temperature ranges 2000 to 2500 C and 1200 to 2000 C, respectively, and (3) columnar grain growth and equiaxed grain growth in UO_2 have been simulated in outpile tests.

In this task; an apparatus will be constructed which will be capable of (1) producing microstructures, similar to the structures obtained inpile, in both pellet and compacted powder fuel specimens, (2) measuring temperatures associated with the structural changes of interest, and (3) performing reliable and accurate calorimetry for thermal conductivity determinations. Initially, existing related technology will be studied in an effort to establish a basis for the conceptual design of the apparatus and to examine the experimental factors influencing the structural changes of interest.

The initial tests will be made on UO_2 pellets so that the performance of the apparatus can be correlated with existing UO_2 structure-temperature correlations and thermal conductivity. After determining the reliability and peculiarities of the equipment and completing the UO_2 tests, investigations on ThO_2-UO_2 will be conducted. Some of these specimens will be fabricated from the same batch of fuel and at the same time as the fuel for the irradiation specimens so that the effects of material and fabrication variables will be eliminated or, at least, minimized. A minimum of two U/Th ratios will be studied.

4.3. Work Accomplished During This Report Period

4.3.1. Summary

During this report period, an attempt was made to define the factors which govern the growth of columnar and equiaxed grains in ceramic fuel rods. This information was used to define the functional requirements of an apparatus capable of producing the desired structures out-of-pile. Several experimental approaches were considered for meeting these requirements, and the most promising approach consistent with current funding was selected. The design of the experimental apparatus was initiated, and some pieces of equipment, materials, and supplies were procured.

4.3.2. Literature Search

A literature search of the related work performed at other installations was made to accomplish two main objectives: to assist in defining the functional requirements of the experimental apparatus and to assess the approaches taken by other investigators to simulate inpile fuel rod structures.

In order to set the functional requirements of the apparatus, consideration must be given to the mechanisms producing the fuel structures of interest. For columnar grain growth below melting temperatures, the most plausible mechanism is the migration of voids up the thermal gradient by a sublimation-condensation phenomenon. The basic premise of this mechanism is that material vaporizes off the hot face and condenses on the cool face of voids that take on a lenticular shape, causing the voids to migrate up the thermal gradient. The rate of migration up the thermal gradient has been treated by MacEwan[8] and DeHalas and Horn[9]. The rate of void migration was shown to increase exponentially with temperature and to be proportional to the temperature difference across the void, the reciprocal of the gas atom density in the void, and the reciprocal of the void thickness. It was also shown that the steep thermal gradient in the fuel during irradiation combined with the highly temperature-dependent migration rates cause the void migration to cease over a narrow increment of radius. Thus, there is a sharp demarcation between columnar and equiaxed grains in irradiated ceramic fuel when the thermal gradient is steep. The treatment by DeHalas and Horn also

provides a basis for evaluating the length of time required for the radius of columnar grains to reach a "steady-state" value (for example, less than a 0.01 cm change in 100 days). For steep thermal gradients (about 8000 C/cm), the columnar grain interface ceases to advance for all practical purposes after about 4 days at temperature. For lower thermal gradients, the time would be greater.

Since the rate of void migration depends on the difference in vapor pressures of the hot and cold faces of the void, it is possible to estimate the difference in the initiation temperatures of columnar grain growth for UO_2 and ThO_2. For a given vapor pressure, the corresponding temperature for ThO_2 is higher than for UO_2. On this basis, it is estimated that the temperature of columnar grain growth is 300 to 400 C higher in ThO_2 than in UO_2.

Considering equiaxed grain growth, MacEwan[10] showed that the grain size of UO_2 can be described by the relationship:

$$D_t^3 - D_o^3 = K_o e^{-Q/RT}(t)$$

where D_t and D_o are average grain sizes at time t and time zero
K_o = constant
Q = grain growth activation energy
R = gas constant
T = temperature
t = time

Lyons, et al.,[7] compared the results of UO_2 grain growth experiments of several investigators including MacEwan. Lyons found a substantial spread in activation energies of the various experiments. Depending on the value selected, the temperature inferred from a particular grain size can vary by several hundred degrees centigrade. The spread in the data appears to be related to variations in sample properties including O/U ratio, porosity, impurity level, initial grain size, and inclusion density. To minimize the effect of variations in sample properties, the outpile temperature correlation tests should be conducted on samples from the same fabrication batch that provides the inpile specimens.

Compressive stress or a compressive stress gradient has been shown by the Canadians[11] to have a significant effect on equiaxed grain growth. It is also possible that compressive stress may influence columnar grain growth. Since the exact role of stress is nebulous at this time, it will be assumed that this effect is the same in both the outpile and the inpile tests.

To summarize, the key factors which should be considered in the design of the Task 04 tests from the standpoint of correlation of fuel structure and temperature are:

1. Initial gas composition of the inpile specimens.
2. Temperature gradient in the inpile samples where the structural changes of interest occur.
3. Heat flux since this governs the ΔT across the lenticular voids.
4. Ability to achieve fuel temperatures in the temperature range of interest.
5. Time at temperature the same as for the inpile tests adjusted for any differences in thermal gradient and heat flux.
6. Inpile and outpile specimens from the same fabrication batch.

In addition to these factors, the Task 04 apparatus must be capable of measuring radial temperature differences in the fuel and be suitable for calorimetric determinations so that the thermal conductivity of the fuel can be determined.

The outpile experience in producing grain growth in UO_2 was assessed. Hausner[12,13], MacEwan[8], and Burdg[14,41] among others performed outpile experiments in which they attempted to produce microstructures in UO_2 similar to those attained inpile. Two types of apparatus were employed. Hausner's apparatus utilized induction heating and consisted of a tungsten susceptor surrounded by a cylinder of UO_2. MacEwan and Burdg used a rod type specimen containing a central tungsten resistance heater. Heat in both devices was removed by a water jacket surrounding the specimen of fuel. The results of their experiments (Table 4-1) reveal their success concerning the growth of columnar grains. The probability of producing columnar grains increases with increasing fuel ID temperatures. At ID temperatures below about 2150 to 2350 C, columnar grains are not likely to be formed. The

temperature for initiation of columnar grains decreases with increasing test time, as predicted by DeHalas and Horn's relationship.

Although columnar grains have been produced in the outpile experiments there has been a virtual lack of a definitive boundary between the columnar and equiaxed grain growth regions produced. It is possible that the absence of a definitive boundary is primarily due to the low thermal gradients inherent in the outpile test approaches used, to the small volume of fuel above columnar grain growth temperatures, and to differences in the properties of the fuel tested. Unfortunately, the thermal gradients and the volume of fuel heated above columnar grain growth temperatures cannot be increased significantly without self-heating. In any event, current experience indicates that correlation of outpile columnar grain growth and temperature is difficult and somewhat inaccurate. Because of this, it is planned to concentrate on temperature correlation in the equiaxed grain growth region. Consideration is also being given to supplementing the gradient structure work with isothermal grain growth experiments in an effort to improve the reliability of the correlation obtained.

Burdg reported that the heaters in his apparatus failed by burnout at temperatures above about 2600 C, whereas MacEwan was able to attain heater temperatures up to about 3150 C. The apparent difference in the two designs which would tend to explain this is that the fuel-heater gap width (cold) in MacEwan's apparatus was about 60 mils, whereas in Burdg's experiment it was less than about 1 mil. This suggests that there is an interaction between the fuel and the heater which causes the early heater failure. It seems important therefore to have a wide gap between the heater and fuel if high fuel temperatures are to be attained, even though the gap ΔT would be greater. The relationship presented in Figure 4-1 shows that the gap ΔT increases rapidly with increasing gap width up to gaps of about 20 mils; then, at greater gap widths, the ΔT doesn't increase very much because of the increasing contribution of radiation heat transfer. It is also important to note that the heater diameters were quite different in the two experiments. Thus, for a given heater power, the heat flux across the fuel-heater gap would be lower for the larger heater diameter (used by MacEwan), and thus the gap ΔT would be less for comparable gap widths.

Table 4-1. Experience Summary

Fuel ID temperature, C	Temperature gradient[f], C/cm	Time at temperature, hr	Temperature for small columnar grains[b], C	Temperature for large columnar grains[b], C	Columnar grains formed?[d]	Device type	Experimenter	Reference No.
2600	2010	0.33	2500	(c)	--	Induction	Hausner	13
2600	2010	2	2210	2320	--	Induction	Hausner	13
2600	1850	6	1900[a]	2145[a]	--	Induction	Hausner	13
2600	2720	6	1850[a]	2050[a]	--	Induction	Hausner	13
2500	3700	3	--	2030/2190[e]	Yes[e]	Hot wire	Burdg	41
2550	2170	3	--	--	Yes	Hot wire	MacEwan	8
2400	1770	0.33	(c)	(c)	--	Induction	Hausner	13
2400	1770	2	2250	2360	--	Induction	Hausner	13
2400	10,000[g]	20	--	1940/2080[e]	Yes[e]	Hot wire	Burdg	41
2420	1930	12	--	--	Yes	Hot wire	MacEwan	8
2350	2680	7	--	--	Yes	Hot wire	MacEwan	8
2140	1500	2	(c)	(c)	--	Induction	Hausner	13
2140	1340	25	(c)	(c)	--	Induction	Hausner	13
2140	1500	25	2200	(c)	--	Induction	Hausner	13
2050	2260	8	(c)	(c)	--	Hot wire	MacEwan	8
2050	1575	25	(c)	(c)	--	Hot wire	MacEwan	8

[a] Estimated.

[b] Temperatures are for onset of columnar grain growth.

[c] None observed.

[d] No distinction between small or large columnar grains and no temperatures given.

[e] Described as "massive grains" by experimenter.

[f] Unless noted otherwise, the temperature gradients were computed from the ID and OD temperatures of the fuel and the fuel radial thickness. In these cases it is estimated that the gradient anywhere along the radius is not significantly different from the reported values.

[g] Temperature gradient in the range of 1400 to 2400 C.

The tungsten resistance-heated devices (used by MacEwan and Burdg) lend themselves reasonably well to thermal conductivity measurements. The cooling jackets and system calorimetry are simple and straightforward. Heater and fuel temperatures can be measured using optical pyrometry and slotted fuel pellets[14]. When heater temperatures approach 2500 C, mass transfer of the fuel tends to plug the sighting holes, thereby causing difficulty in reading the heater temperatures. In addition, corrections for emissivity of the tungsten and the fuel must be made to allow for the lack of black-body conditions in the sight holes[8,14,15]. Since these corrections are, at best, approximations for the actual radiative conditions existing in the sight wells, it would be highly desirable to run a calibration experiment having a complete mockup of the sighting wells, in which thermocouples could be used as the "reference standard".

The induction-heated device (used by Hausner) was also briefly examined. The induction heater has the primary advantage of less sensitivity to local resistance changes, and therefore it should be more reliable than the resistance heater is. For example, total fracture of the susceptor would not affect the power output of the induction-heated device, but fracture of the resistance heater would cause it to stop functioning. To more than offset this advantage, there are several disadvantages. Power requirements are large so that the length of the specimens would have to be kept short (less than 1 inch) to make the power requirements reasonable. Design of the cooling jacket would be quite difficult, if calorimetry is to be performed, because the materials of construction would probably have to be nonsuscepting (nonconducting). Sighting wells in the fuel for optical pyrometry would have to be axial and would require that the diameter of the fuel specimen be large enough (greater than about 2 inches) to accommodate the sight holes. This would move the HF coil further away from the susceptor and reduce the coupling.

Consideration was also given to a tungsten resistance-heated device in which the heater surrounds a fuel cylinder and the heat is extracted on the ID of the specimen. A similar device was developed by Rasor and McClelland[16] for thermal property measurements at high temperatures, except that they used a graphite helical heater which was externally insulated with carbon wool and carbon black. A bayonet type heat sink was used for calorimetry. Specimen OD temperature was

measured by optical pyrometry through sight holes which penetrated the insulation and the separations in the helix. Temperatures inside the specimen were optically measured using axial sight holes formed in the end of the specimen.

The large heater surface of the externally heated specimen makes it possible to attain very large ΔT's in the fuel while having a low ΔT across the heater-fuel gap. For example, it appears possible to operate the heater at about 2900 C while operating the OD of the fuel at 2700 C. This is a major advantage since the higher temperatures enhance the growth of columnar grains. The disadvantages of this approach lie in the design of the radiation shields, heater, and pyrometry and in the cost of materials. Because of the low resistance of a tubular tungsten heater, the current requirements exceed about 2000 amperes for a 2.5-inch-OD heater, neglecting heat losses. Heat losses could increase the current requirements 25 to 50%. Thus, a ribbon or grid type heater would be required to obtain increased heater resistance. This, in turn, would require that the fuel (pellet or powder) be placed inside a tungsten tube for containment. Temperatures of the fuel would necessarily have to be measured optically using axial sight holes, thereby requiring that the fuel thickness be on the order of 1 inch. Penetration of the insulation, radiation shields, heater, and cladding from the side would not be practical for temperature measurement primarily because of cost and alignment problems at temperature.

4.3.3. Apparatus Design

Based on the analysis of the literature survey results, a decision was made to use the axial tungsten resistance heater approach used previously by MacEwan and Burdg because this approach appeared capable of meeting the functional requirements reasonably well and its cost of fabrication and operation appears more compatible with Task 04 funding. An attempt will be made to combine the best features of each of the previous experiments in an effort to maximize the temperature capability of the apparatus.

The initial design effort was focused on the design of the specimen. The objective was to first determine the heater, fuel, and insulation diameters which would provide the desired flexibility of

operation but at the same time maximize the temperature performance. The following parameters were selected:

Heater diameter	0.250-inch OD
Fuel cylinder	0.870-inch OD by 0.370-inch ID
Fuel-heater gap	0.060 inch
Insulation	ZrO_2 (sintered)
Fuel	UO_2 pellets

Thermal calculations were performed to determine the heat rating necessary and the fuel outer surface temperatures for various fuel inner surface temperatures. The heater temperature was set at 3000 C as the maximum attainable without excessive heater vaporization and reduced reliability. Since an axial gap approximately 60 mils in thickness exists between the heater surface and the inner fuel surface, heat will be transferred across this helium-filled gap by both radiation and conduction. The equation used to determine the required heat rating is:

$$\frac{q}{\ell} = \frac{2\pi k_{He} \Delta T}{\ell n \frac{D_2}{D_1}} + \frac{A_1 \sigma}{\frac{1}{\epsilon_1} + \frac{A_1}{A_2}\left(\frac{1}{\epsilon_2} - 1\right)}\left[\left(\frac{T_1}{100}\right)^4 - \left(\frac{T_2}{100}\right)^4\right]$$

where

$\frac{q}{\ell}$ = linear heat rating

k_{He} = thermal conductivity of He gas

ΔT = temperature drop across He filled gap

D_1, D_2 = inner and outer diameters of the annular gap

A_1 = surface area of heater wire

A_2 = fuel inner surface area

σ = Stefan-Boltzmann constant

ϵ_1, ϵ_2 = emissivities of tungsten and uranium dioxide

T_1, T_2 = temperatures of the heater surface and fuel inner surface

The results of this calculation are shown in Figures 4-2 and 4-3. Because of possible interactions between the fuel and the insulation, the temperature of the fuel OD surface will probably be limited to between 1500 and 2000 C. Figure 4-3 shows that the maximum fuel ID temperature will be limited to 2600 to 2700 C. The corresponding

power requirement will be 5.8 to 7.5 kw/ft (Figure 4-2), and the corresponding temperature gradient in the fuel will be about 1300 C/cm.

Calculations determined the insulation thickness required to produce the desired fuel inner surface temperature. Zirconium dioxide was chosen as the insulation material. The outer surface of the insulation will be maintained at about 100 C. An insulation thickness of 0.375 inch will be adequate to maintain the fuel inner surface temperature as high as 2700 C.

The radial temperature distribution across the fuel specimen was calculated for a fuel ID surface temperature of 2700 C and a heat rating of 5.8 kw/ft. The thermal conductivity, as determined by Duncan[17], for UO_2 pellets of 95% theoretical density is an "effective" thermal conductivity determined from the expression

$$k_{eff} = \frac{\int_{T_1}^{T_2} k\,d\theta}{T_2 - T_1} .$$

The results are plotted in Figure 4-4. It was estimated (Section 4.3.2) that the initiation temperature for columnar grain growth in ThO_2 is about 300 to 400 C higher than in UO_2. Taking the temperature for columnar grain growth in UO_2 as the median of the values (excluding the 0.33-hour data) reported in Table 4-1, the initiation temperature for columnar grains in ThO_2 is about 2400 C. Figure 4-4 shows that 0.085 inch of the fuel thickness is above this temperature.

The cooling jacket has been designed. Calculations determined the heat removal parameters for various water flow conditions. Coolant conditions must provide an adequate temperature rise in the coolant water to allow accurate calorimetry measurements. Bulk boiling on the specimen cladding is to be avoided to maintain uniform heat removal over the entire specimen surface. A flow rate of 10 gpm will produce a temperature rise of approximately 2.5 C in the coolant water and maintain the clad surface below 90 C. An inlet water temperature of 2.1 C was assumed for the coolant calculations. A differential temperature transducer will be used for measuring the ΔT in the water. The quoted accuracy of this device is ± 0.039 C.

The power characteristics of the 0.25-inch-diameter tungsten heater were examined to determine the relative advantages of a solid versus a tubular heater. In the case of a tubular heater with a 30-mil wall operating at 1900 and 3400 w/cm (see Figure 4-2 for corresponding fuel ID temperatures), the power characteristics are 8 volts with 490 amperes and 11 volts with 650 amperes, respectively. With a solid (rod) heater, the power characteristics for the 3400 w/cm operation are 6.9 volts and 995 amperes. Selection of the d-c power supply is being made on the basis of these requirements.

The thermal expansion of both the fuel and the insulation pellets was calculated to determine the hot and the cold pellet profiles so that sighting wells for the optical pyrometer can be properly located. The fuel and the insulation pellet lengths and sight well locations are shown in Figure 4-5.

4.4. Planned Work for Next Report Period

During the next report period, the design of the apparatus and procurement of materials and equipment will be completed. Also, component fabrication and assembly of the apparatus will be finished. The first specimen will be fabricated and made ready for the initial experimental runs.

Figure 4-1. Heater Surface Temperature Vs Heater-Fuel Gap Thickness

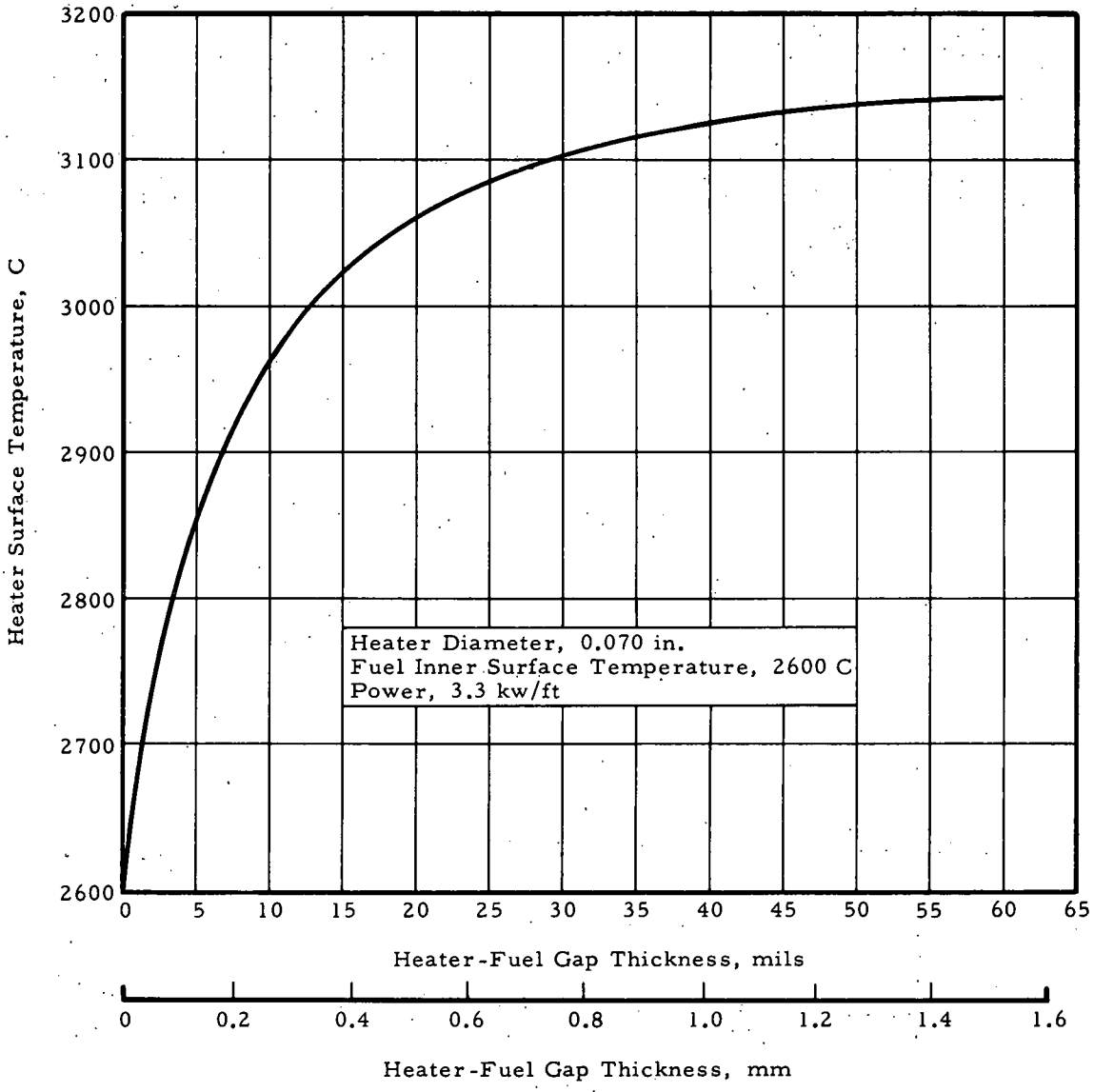

Figure 4-2. Heat Rating Required Vs Various Fuel Inner Surface Temperatures

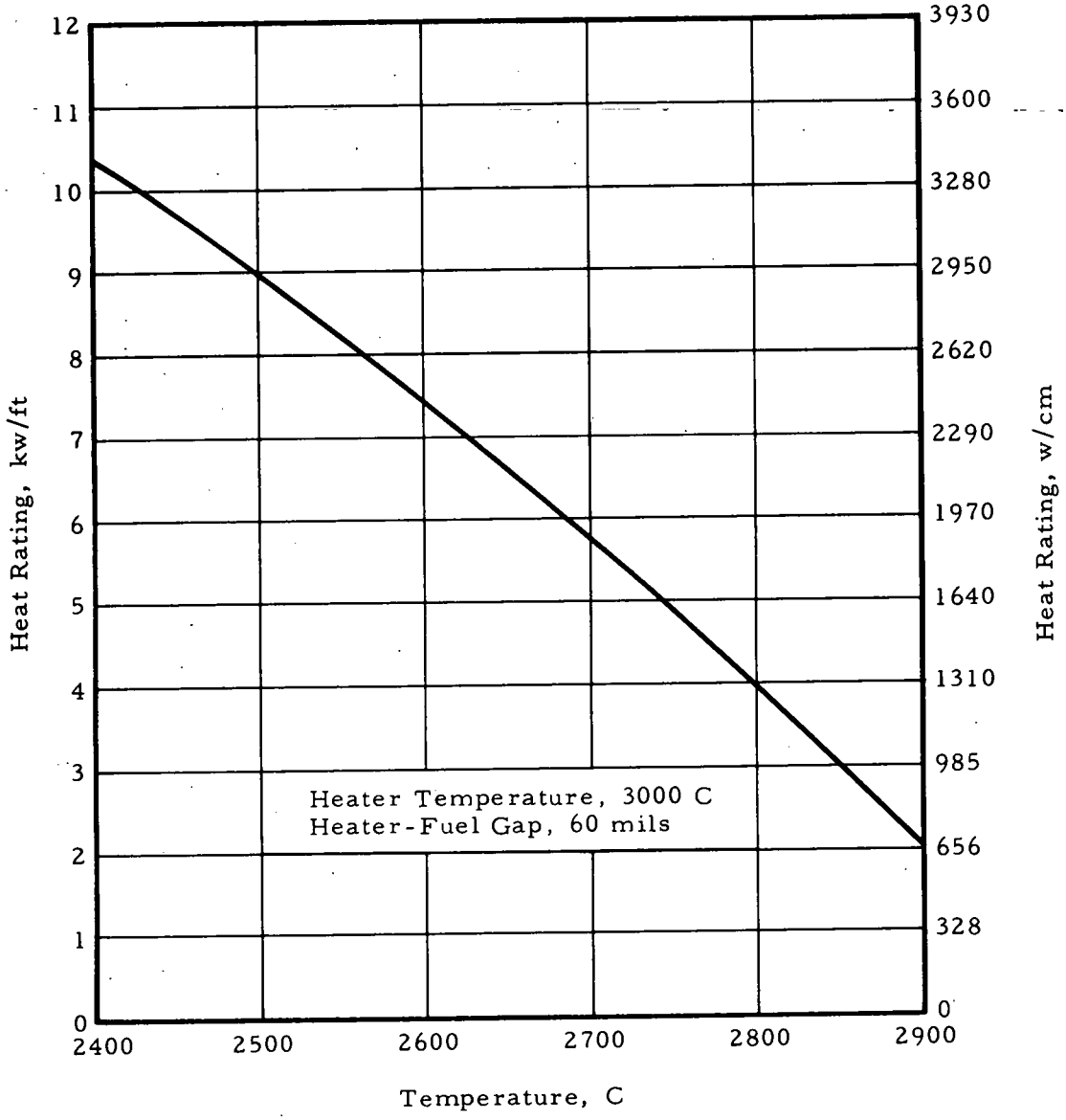

Figure 4-3. Fuel Outer Surface Temperature Vs Fuel Inner Surface Temperature

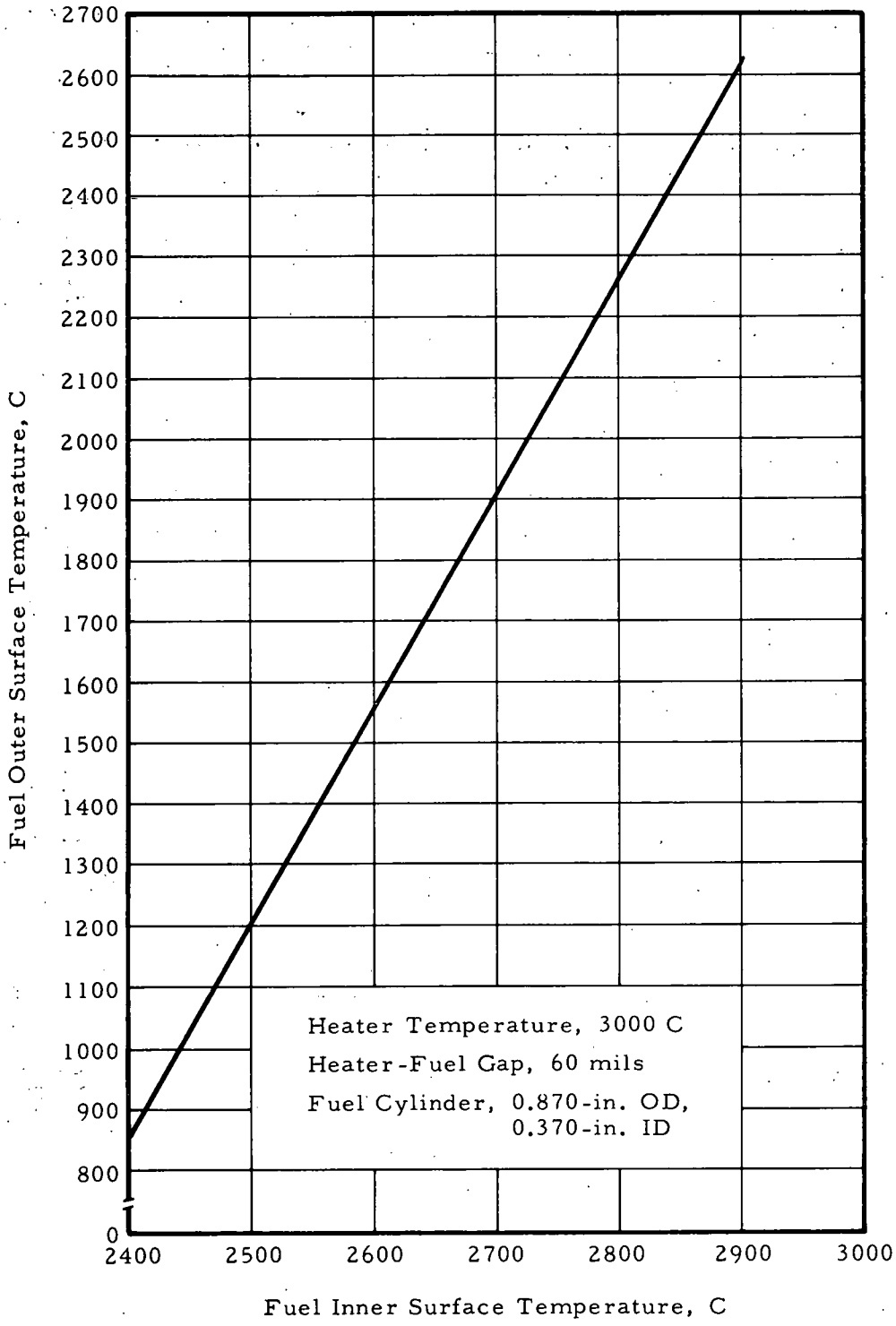

Figure 4-4. Radial Temperature Profile of Urania Pellet

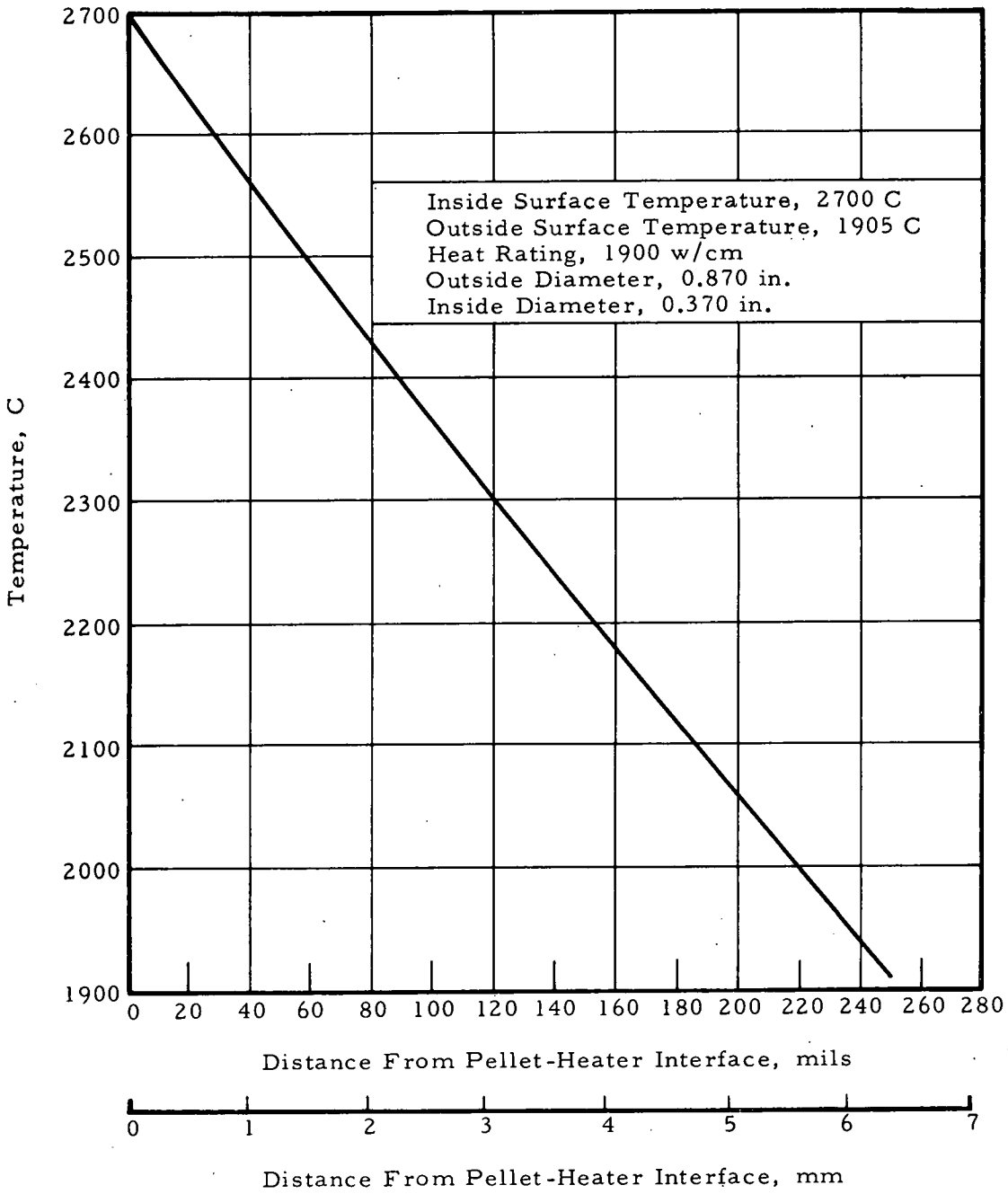

Figure 4-5. Specimen Tube Thermal Simulation Device

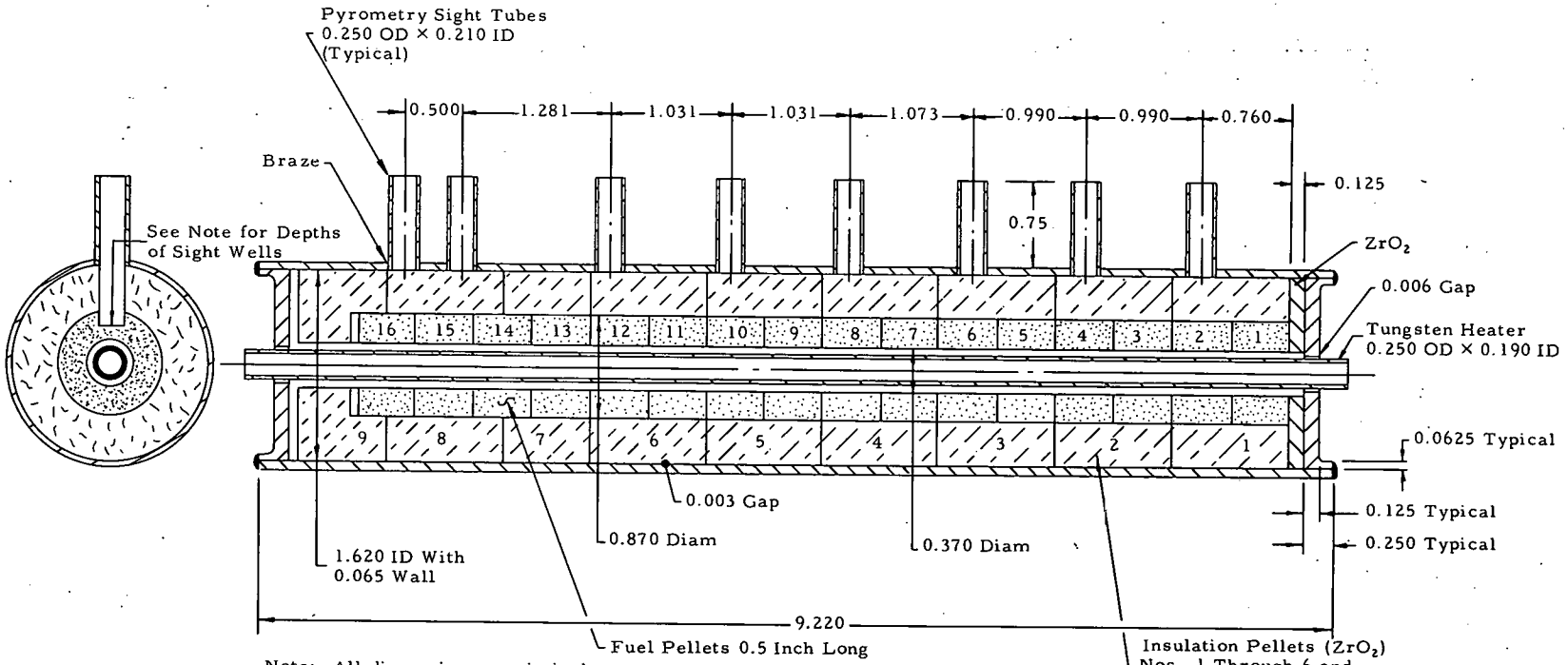

Note: All dimensions are in inches.
The fuel pellets will be slotted as follows:

Pellet No.	Slot depth
2	Inner fuel (heater) surface
4	Intermediate
6	Intermediate
8	Inner fuel (heater) surface
10	Intermediate
12	Outer fuel surface
14	Intermediate
15	Inner fuel (heater) surface

5. IRRADIATED FUEL THERMAL CONDUCTIVITY — TASK 05

(W. R. DeBoskey, Task Leader; L. B. Gross)

5.1. Task Objective

The objective of this task is to obtain the thermal conductivity of thoria-urania fuel to the melting point by inreactor self-heating. The correlation of temperature with structure alterations determined in the Unirradiated Fuel Thermal Conductivity Task (Task 04) will be necessary to establish the temperatures achieved at particular locations in the irradiated specimens of this task. Comparisons will be made between thermal conductivity values determined by the electrical heating method of Task 04 and by the inreactor self-heating of this task.

5.2. Task Description

Through the use of nuclear self-heating, the "heat rating ($\int k d\theta$) versus temperature" relationship for ThO_2-UO_2 to the melting point of the oxide will be developed. Experiment parameters will be chosen to bracket the melting point (3 specimens) and, if possible, to bracket columnar grain growth (2 specimens). This task will be accomplished by selective predetermined loading of four inreactor capsules containing twenty fuel rod specimens as follows:

1. Five specimens of nominal 5 wt% UO_2 in ThO_2, pellets.
2. Five specimens of nominal 5 wt% UO_2 in ThO_2, vibratory compacted sol-gel powder.
3. Five specimens of nominal 10 wt% UO_2 in ThO_2, pellets.
4. Five specimens of nominal 10 wt% UO_2 in ThO_2, vibratory compacted sol-gel powder.

Properties such as density and isotopic composition will be initially determined for all fuel batches. Sources and batches of specimen

material will be the same as used in the gas release experiments of Tasks 06 and 07.

Individual capsule irradiation will be of short duration (approximately 3 or 4 days) during which time constant neutron flux will be attempted. The inreactor space and capsule equipment console will be shared with Task 07 capsules. Capsule instrumentation will be neutron monitors and thermocouples if practicable.

Postirradiation examination will be initiated before additional Task 05 capsules are inserted. The postirradiation examination of the twenty specimens will determine the relationship between temperature and heat rating ($\int k d\theta$) for bulk and powder materials for the two urania compositions investigated. Analysis of characterization and operating data as well as radiochemical, isotopic, and ceramographic examinations will be accomplished. Assigning the temperature profile to the fuel specimen is a prerequisite and is achieved by noting the locations of various temperature-associated structural changes such as melting and changes in grain morphology.

Differentiation of the heat rating integral ($\int k d\theta$) with respect to temperature will yield thermal conductivity as a function of temperature. Thermal data obtained from pellets will be utilized to establish the general shape and magnitude of "$\int k d\theta$" and thermal conductivity versus temperature curves. Application of sol-gel experimental data to the general curve will lead to specific knowledge of the thermal conductivity of sol-gel powder.

5.3. Work Accomplished During This Report Period

5.3.1. Summary

Work performed during this initial period included writing the detailed work statement and establishing the capsule design approach. It is necessary in these designs to maintain cognizance of the task objective, the BAWTR operating characteristics, and limitations imposed by the BAWTR license. Since the BAWTR is a new reactor and, therefore, not fully characterized, it is necessary to assume some operational characteristics such as the magnitude and variation of neutron flux and coolant availability.

The general approach is to develop a design concept and then adapt it to the particular requirements of the BAWTR system. The first design had a temperature-controlled fuel surface. Since calculation of the temperature profile could not be accomplished, this concept was discarded. A second design minimizing fuel surface temperature was then developed.

5.3.2. First Design

The basic design concept must be in accordance with the double capsule requirement of the BAWTR license for irradiation of fuel or liquid metals. To accomplish this requirement, a clad cylinder of fuel located in an outer capsule containing helium as a thermal transfer medium was proposed. Electrical heaters were included to compensate for fuel surface temperature fluctuations due to varying heat flux. This design is illustrated schematically in Figure 5-1.

The Fourier thermal conduction equation, as applied to a helium annulus, is described by the curves in Figure 5-2. (Radiant heat transfer is not applicable in this instance due to the relatively low temperature and small thermal gradient involved.) The radial thickness of the helium annuli on either surface of the cylindrical heater must be kept small so as to maintain a small thermal gradient. However, the movements due to thermal expansion of the heater and capsule walls would shift the helium gaps, which in turn would alter the temperature profile. Calculation of this temperature profile could not be accomplished since it was not possible to reasonably determine the thermal expansion of the capsule components due to this temperature profile uncertainty.

An additional difficulty encountered in this design is associated with electrical heater performance. A heater output of approximately 900 watts per cm at the reactor midplane for specimen heat fluxes in the order of 80 watt/cm^2 is required to compensate for the expected ±25% variation in specimen heat input. As a result of the restricted dimensions, a 440-volt input is required. However, 440-volt single-phase equipment is difficult to procure.

For these two reasons—an unpredictable thermal profile and difficult procurement of a suitable heater—this design was abandoned, and a simpler approach was developed.

5.3.3. Second Design

The second design avoided the shortcomings of the first design by limiting rather than controlling the fuel surface temperature. By minimizing the fuel surface temperature, temperature fluctuations caused by input heat variations are reduced. Therefore, although there is no external control, the possible variation in fuel temperature is sufficiently small to approach the desired effect of temperature control. To accomplish this, the thermal resistance surrounding the fuel surface must be reduced while maintaining the license requirement of a double capsule. Thus, a cylinder of fuel in a double capsule having no additional components in the assembly was proposed. The two capsules are separated by a helium gap, which is only large enough to allow assembly. This is illustrated in Figure 5-3.

Maintenance of a constant temperature at the fuel surface requires dimensional stability of the capsule walls. That is, plastic deformation in the capsule walls must be precluded. This may be accomplished by selecting a construction material that has a yield strength greater than the combined thermal and internal gas pressure stresses imposed upon it.

5.3.4. Design Adaption to BAWTR

The schematic diagram of the BAWTR core is presented in Figure 5-4. The center hole C-5 and the corner reflector hole RL-2 were selected as tentative test sites based on flux stability, flux magnitude, and coolant availability. Only the corner and center irradiation sites may be reworked to expand their diameters, and RL-2 has the highest neutron flux at a corner. Nuclear analysis shows that enlargement of the existing reflector hole RL-2 to 2.25 inches in diameter does not seriously alter the predicted nuclear performance of the BAWTR. Though the neutron flux in RL-2 is less than in C-5, it is sufficient to accomplish the experiment. Therefore RL-2 (enlarged) has been selected as the tentative radiation site.

The fuel diameter was maximized to reduce the specific power rating for a desired heat rating ($\int kd\theta$). This reduces the required number density of fissile atoms for a given neutron flux, which allows the use of a fuel low in UO_2. This reduced UO_2 requirement enhances

the possibility of fuel manufacture by the sol-gel process and maintains the U/Th ratio within the range of projected commercial usage. A second result of maximizing the fuel diameter is the reduction of heat flux (Q/A) at the capsule surface. There is a corresponding reduction of capsule surface temperature, which is necessary to avoid local boiling. (Boiling or void manufacture is prohibited by the BAWTR operating license.)

The most probable BAWTR operating conditions are as follows:

Condition	Nominal value	Maximum or scram point value
Inlet water temperature	54 C	57 C
Primary water flow rate	259 liters/sec	220 liters/sec
Core water pressure drop	457 gm/cm^2	--
Gamma heating	2 watts/gm	3 watts/gm
Power	6 MW-t	7.2 MW-t

If the full pressure drop of 457 gm/cm^2 is realized, the primary water flow rate can be maximized. Neutron flux variations during operation together with variations in the number density of fissile atoms will determine the heat rating variation. This information is presented below along with other design calculational uncertainties.

Condition	Nominal value	Maximum or scram point value
Coolant flow rate	4.2 liters/sec	3.5 liters/sec
Heat rating ($\int kd\theta$)	As required (Table 5-1)	125% of requirement
Film drop variation[18]	Modified Colburn	0.8 × Modified Colburn

The specimens for this task will be distributed in capsules in accordance with Table 5-1. The positions in the capsules were selected to optimize space utilization within the neutron flux cosine

distribution and to minimize the number of fissile atom enrichments needed. These locations are further described in Figures 5-5 and 5-6.

5.4. Planned Work for Next Report Period

Using the BAWTR operating conditions stated above, the second design will be completed for the safeguards report. After neutron flux information from high power operation of the reactor is obtained, specimen fissile atom enrichments will be determined. Procurement of long-lead-time capsule materials will commence.

Table 5-1. Capsule Loading Scheme

Capsule number	Specimen number[a]	Specimen type	Specimen position, inches[c]	UO_2 content, wt%	Heat rating, $\int kd\theta$, w/cm	Approximate fuel center temperature, C	Enrichment (fission atom number density)
05-1	1	Pellet[b]	+13, +10	5	49.9	2260	E-1
	2	Powder	+10, + 2	10	80	Melting	E-1
	3	Pellet	+ 2, - 1	5	106	Melting	E-1
	4	Pellet	- 1, - 4	10	78	Melting	E-2
	5	Pellet	- 4, - 7	10	72.5	3150	E-2
	6	Powder	- 7, -15	5	45	2850	E-2
05-2	1	Pellet[b]	+13, +10	10	49.9	2260	E-1
	2	Powder	+10, + 2	5	80	Melting	E-1
	3	Pellet	+ 2, - 1	10	106	Melting	E-1
	4	Pellet	- 1, - 4	5	78	Melting	E-2
	5	Pellet	- 4, - 7	5	72.5	3150	E-2
	6	Powder	- 7, -15	10	45	2850	E-2
05-3	1	Pellet	+12, + 9	10	58.5	2620	E-1
	2	Powder	+ 9, + 1	10	55	3200	E-3
	3	Powder	+ 1, - 7	5	58	Melting	E-3
	4	Powder	- 7, -15	5	25	1900	E-4
05-4	1	Pellet	+12, + 9	5	58.5	2620	E-1
	2	Powder	+ 9, + 1	5	55	3200	E-3
	3	Powder	+ 1, - 7	10	58	Melting	E-3
	4	Powder	- 7, -15	10	25	1900	E-4

[a] Specimens numbered from top to bottom of capsule.

[b] Thermocouple-instrumented specimen.

[c] Top and bottom positions of specimen relative to BAWTR core midplane.

Figure 5-1. First Design: Axial Section Schematic Diagram

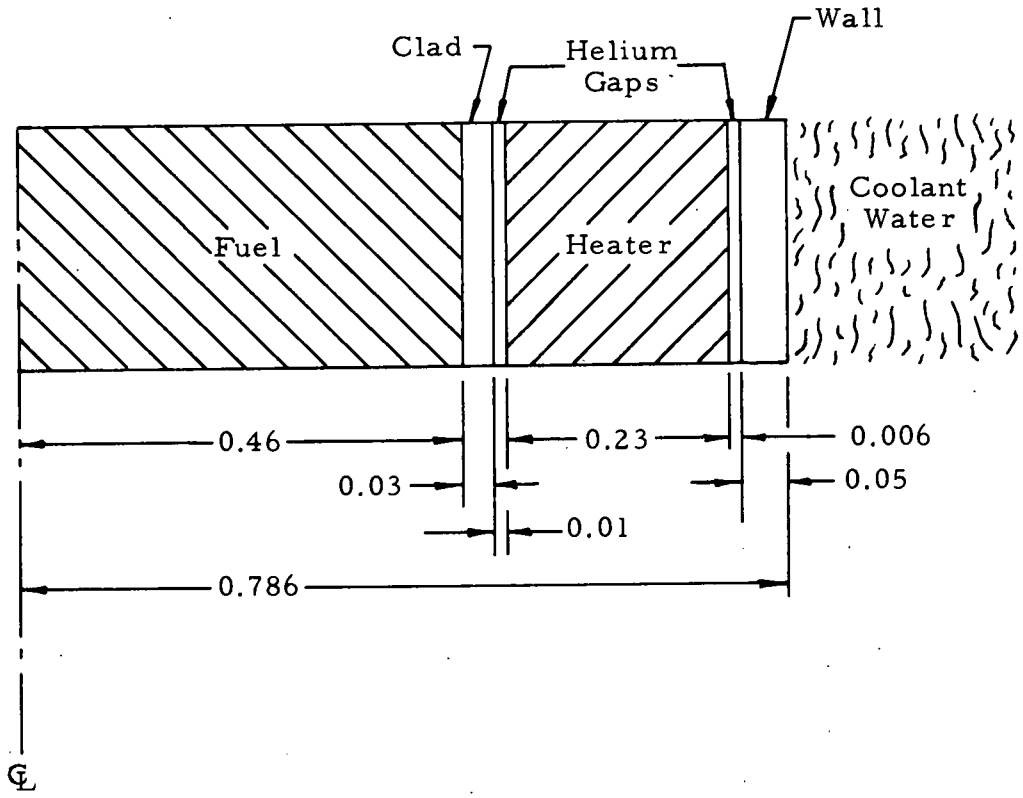

Note: All dimensions are in inches.

Figure 5-2. Thermal Conduction Across an Annular Helium Gap

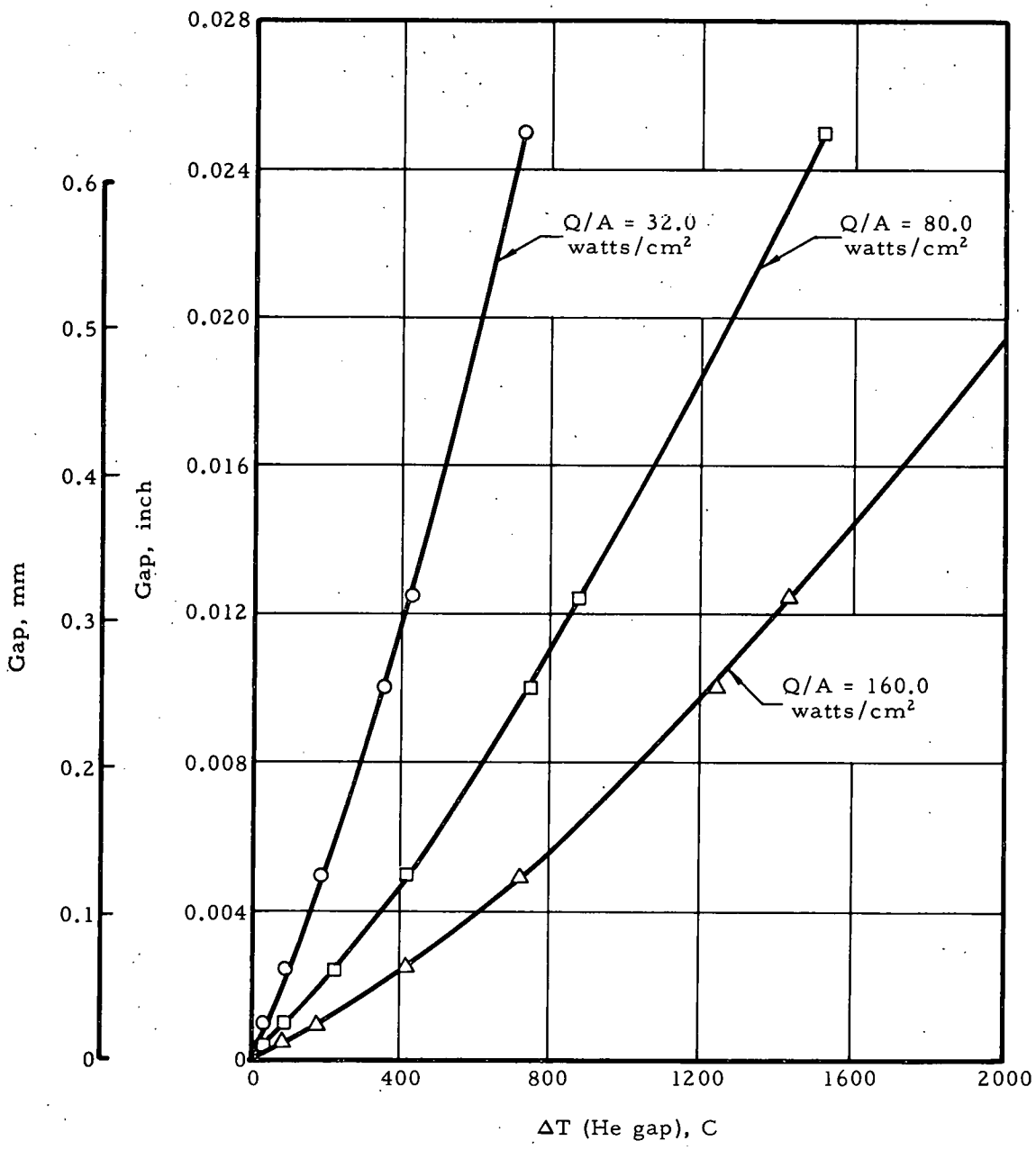

Figure 5-3. Second Design: Axial Section Schematic Diagram

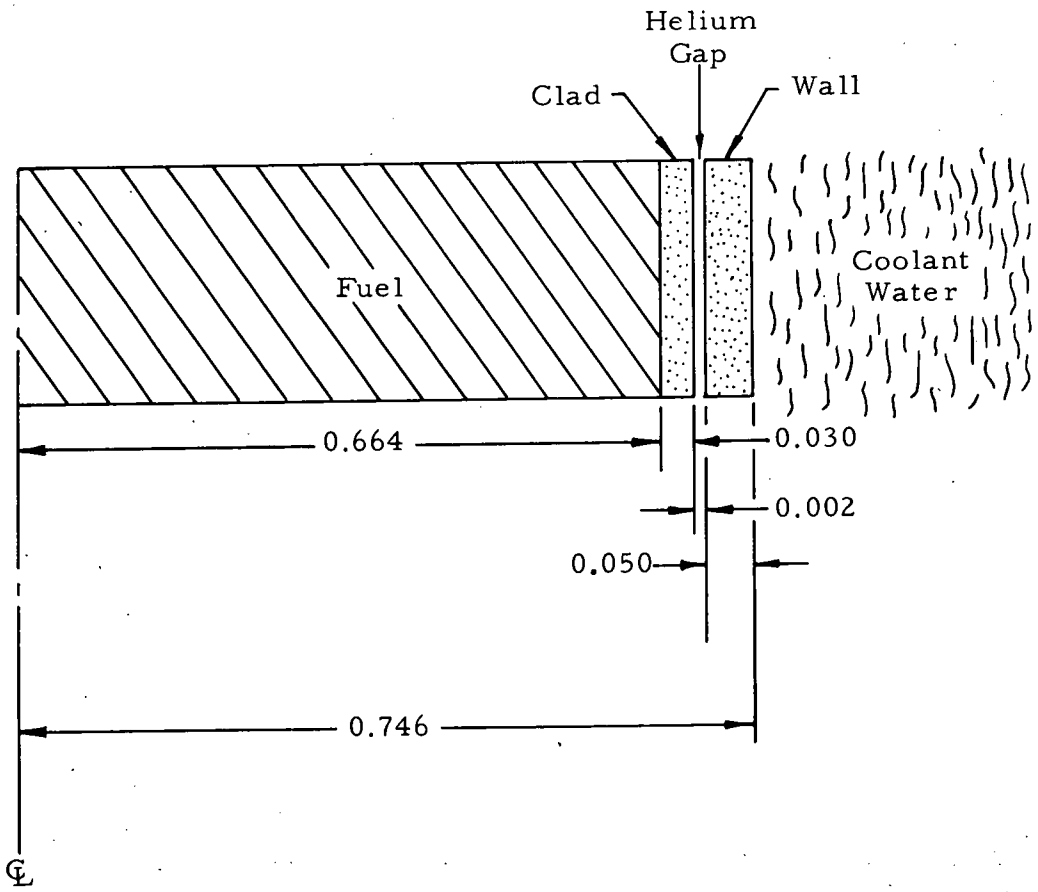

Note: All dimensions are in inches.

Figure 5-4. BAWTR Core Schematic Diagram

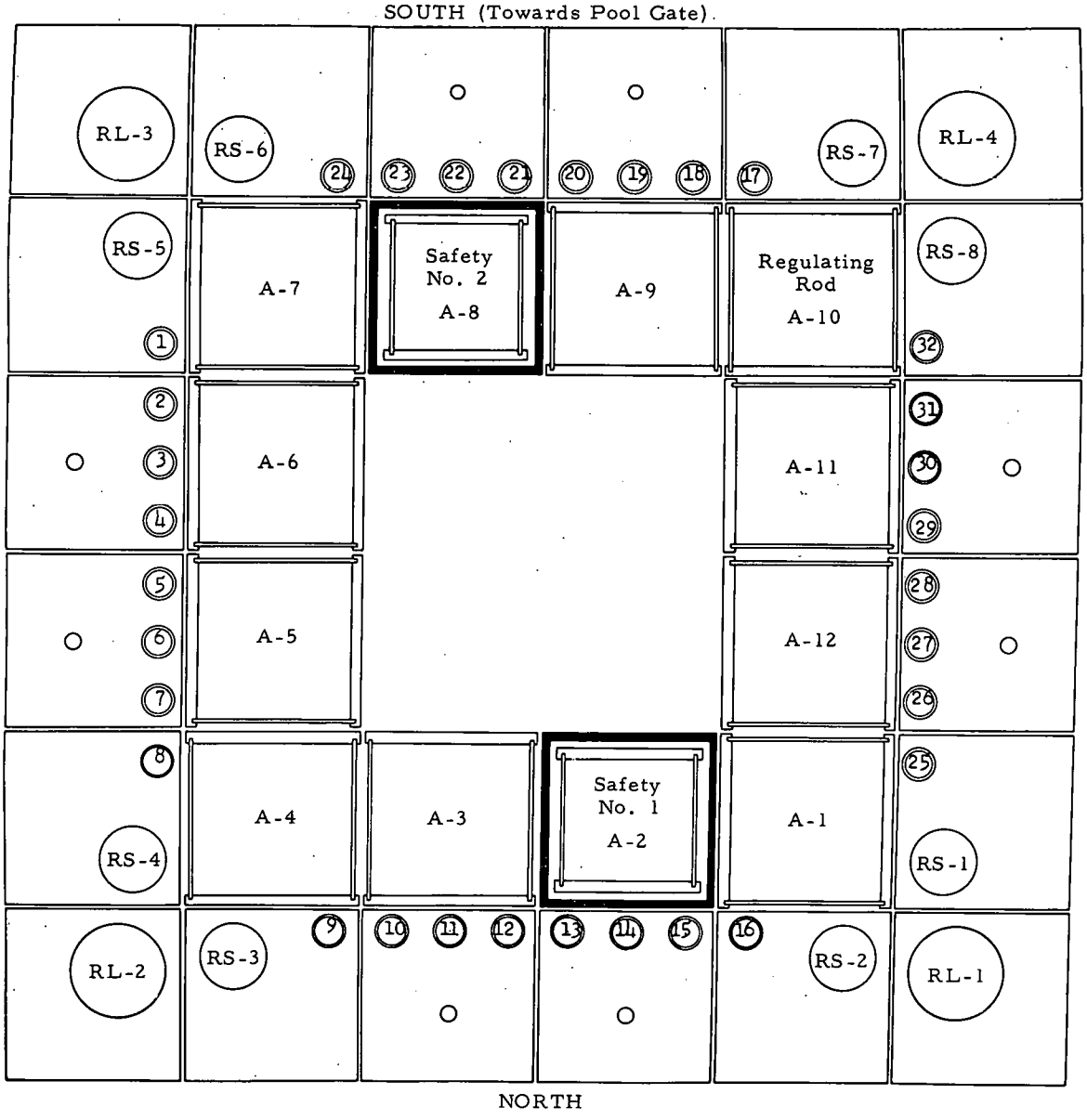

Figure 5-5. Specimen Positions Within Capsules 05-1 and 05-2

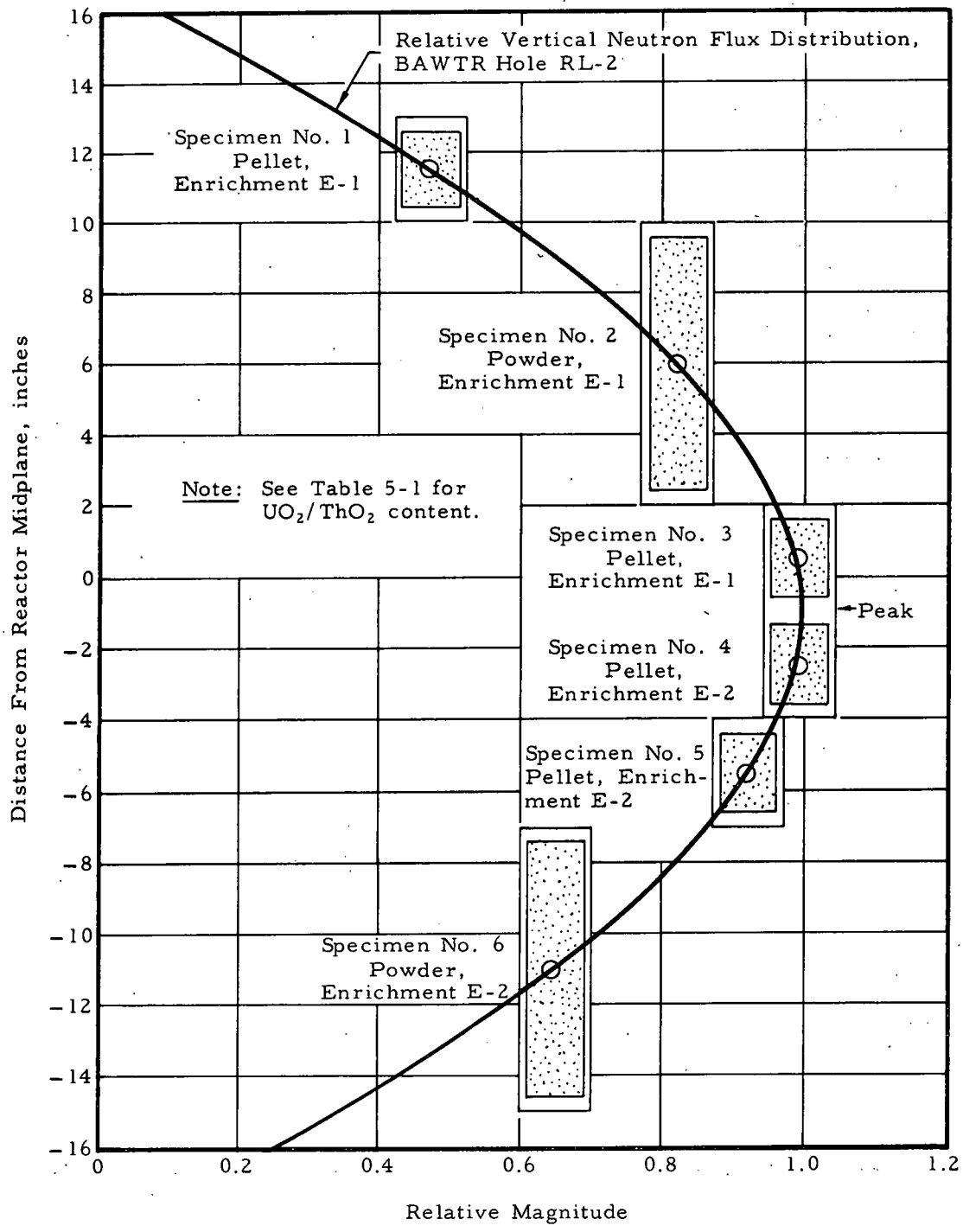

Figure 5-6. Speciman Positions Within Capsules 05-3 and 05-4

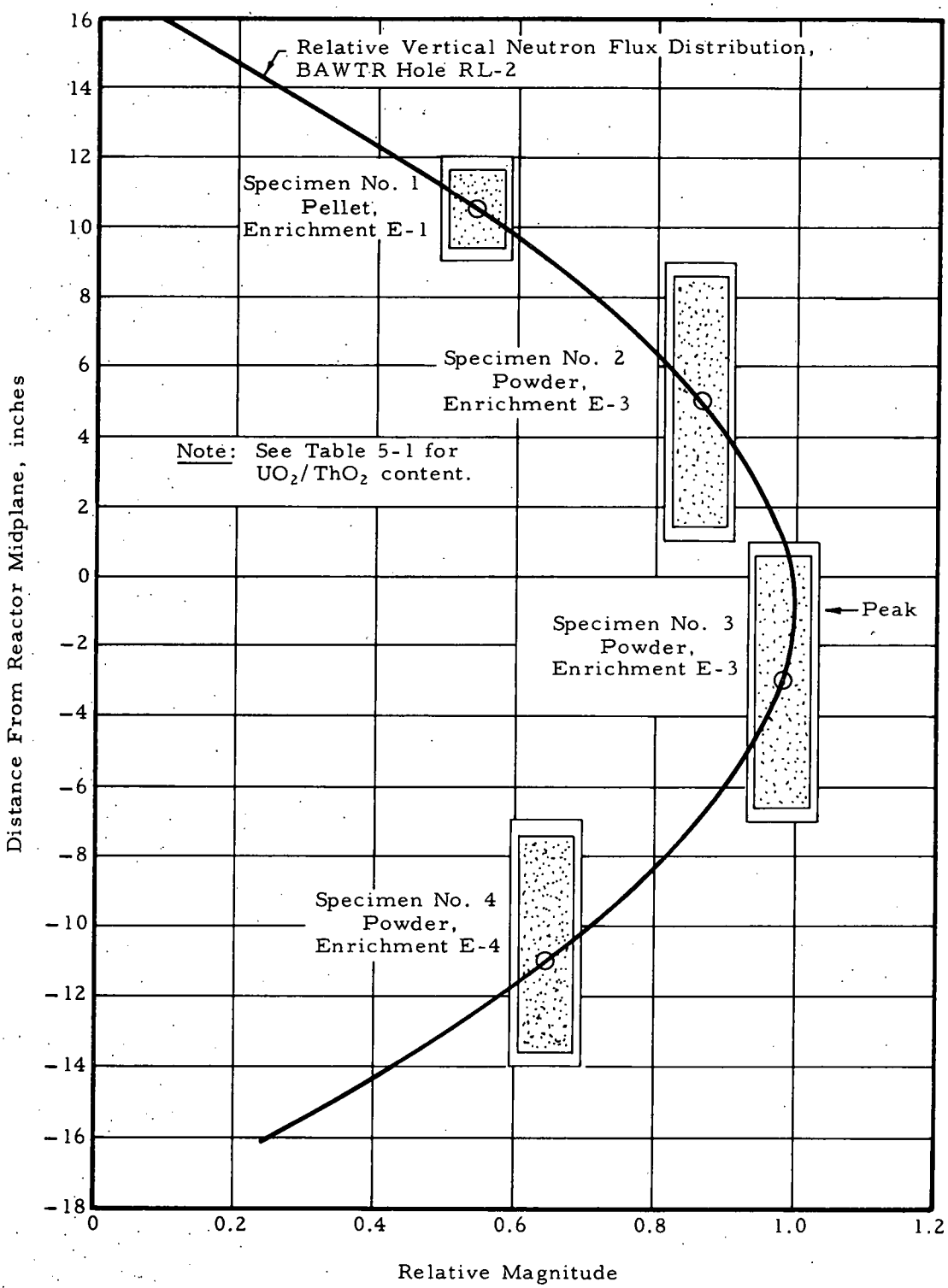

6. DYNAMIC INPILE FISSION GAS RELEASE EXPERIMENT — TASK 06

(W. R. DeBoskey, Task Leader; L. B. Gross)

6.1. Task Objective

The objective of this task is to determine the internal gas pressure in a thoria-urania fuel rod as a function of time during reactor operation. The effect on fission gas release of initial and terminal operation at sufficiently high power to significantly alter the grain structure will be examined.

6.2. Task Description

By inreactor monitoring, the internal gas pressures of a series of ThO_2-UO_2 fuel rods will be determined during reactor operation. Four capsules will be irradiated: two capsules to undergo a power burst at the beginning of the inreactor exposure, and the remaining two capsules to undergo a power burst at the end of the inreactor exposure. Four specimens, one to be inserted in each capsule, will have nominal 5 wt% UO_2 in ThO_2 in the following forms:

1. Pellet (initial burst).
2. Pellet (final burst).
3. Vibratory compacted sol-gel powder (initial burst).
4. Vibratory compacted sol-gel powder (final burst).

Properties such as density and isotopic composition of the specimen materials and operating characteristics of the detection systems will be determined. Specimen material sources and batches will be the same as those used for Tasks 05 and 07.

Capsules will be irradiated individually for approximately 60 days. Gas pressure and neutron flux will be recorded as a function of time.

Power bursts will exceed normal operation to that degree required for extensive recrystallization or center melting.

Postirradiation examinations will include analyses of preirradiation data and operating data, gas sampling, radiochemistry, and ceramographic examinations. Data obtained from pellet investigations will provide value limits for the more-difficult-to-analyze powder data. Samples of these specimens will be made available for postirradiation gas permeability measurements under Task 02.

6.3. Work Accomplished During This Report Period

Work performed during this initial period included development of the detailed work statement and general consideration of the instrumentation system.

To determine internal gas pressure in a fuel rod as a function of time during reactor operation, several devices were considered; of those available, the null-pressure switch (Figure 6-1) appears to be the most suitable. This instrument operates by continuous measurement of back-pressure applied to a diaphragm to balance the internal pressure developed in the fuel rod. There is only a slight increase in fuel rod volume, so that small quantities of released gas can produce significant pressure changes. The tentative instrumentation system is shown schematically in Figure 6-2. Preliminary approval by the BAWTR Safeguards Committee was obtained for this instrumentation system. A bench model of the system is being constructed to obtain a better understanding of the problems involved in its operation.

6.4. Planned Work for Next Report Period

Since the capsules of this task are to be similar in many respects to the capsules of the thermal conductivity task, the design of these capsules will not be started until the Task 05 capsules are fully formulated. Bench testing of the instrumentation system will continue until the system is perfected and reliability is ascertained.

Figure 6-1. Null Pressure Switch Schematic Diagram

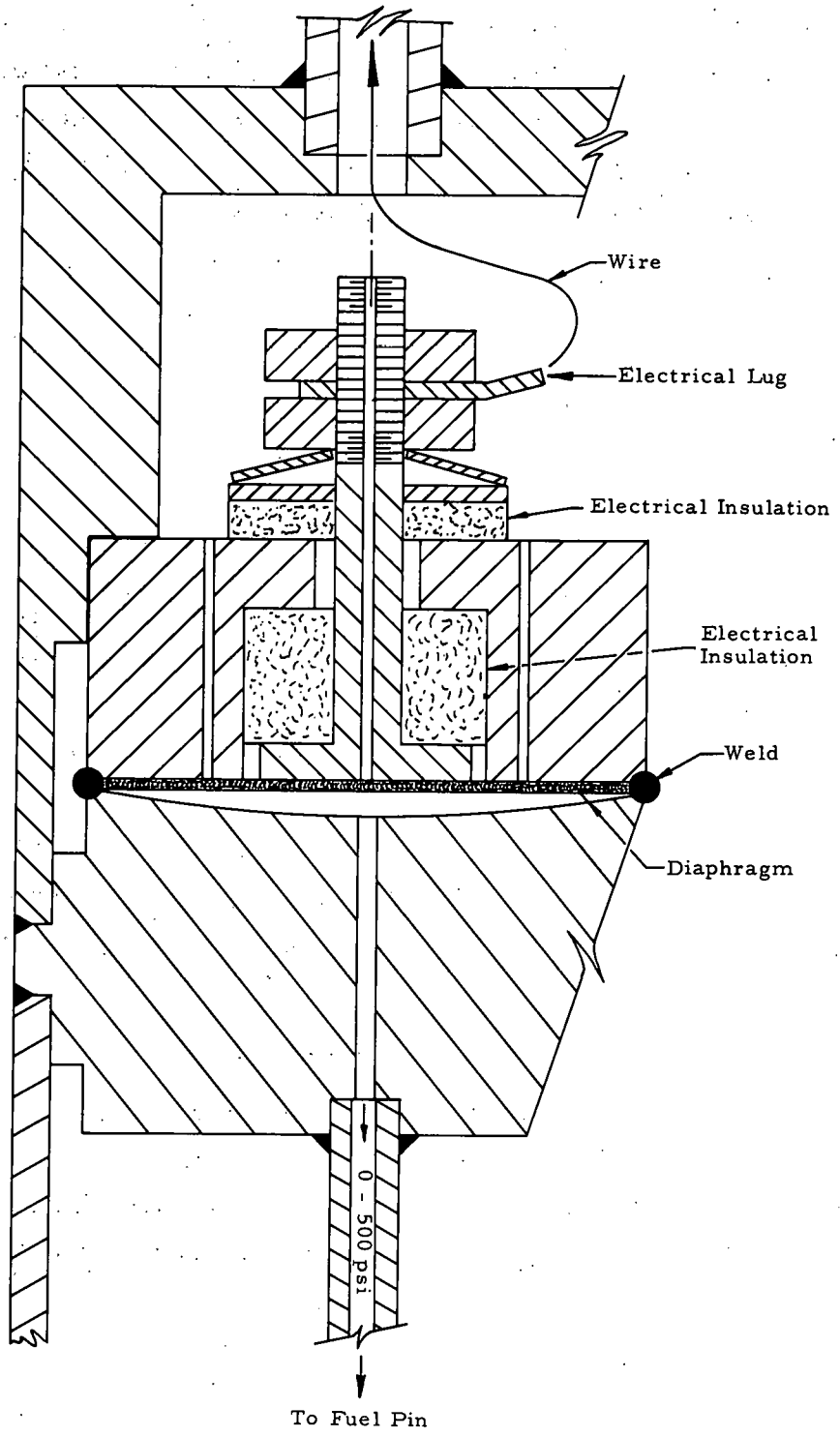

Figure 6-2. Instrumentation System Flow Diagram

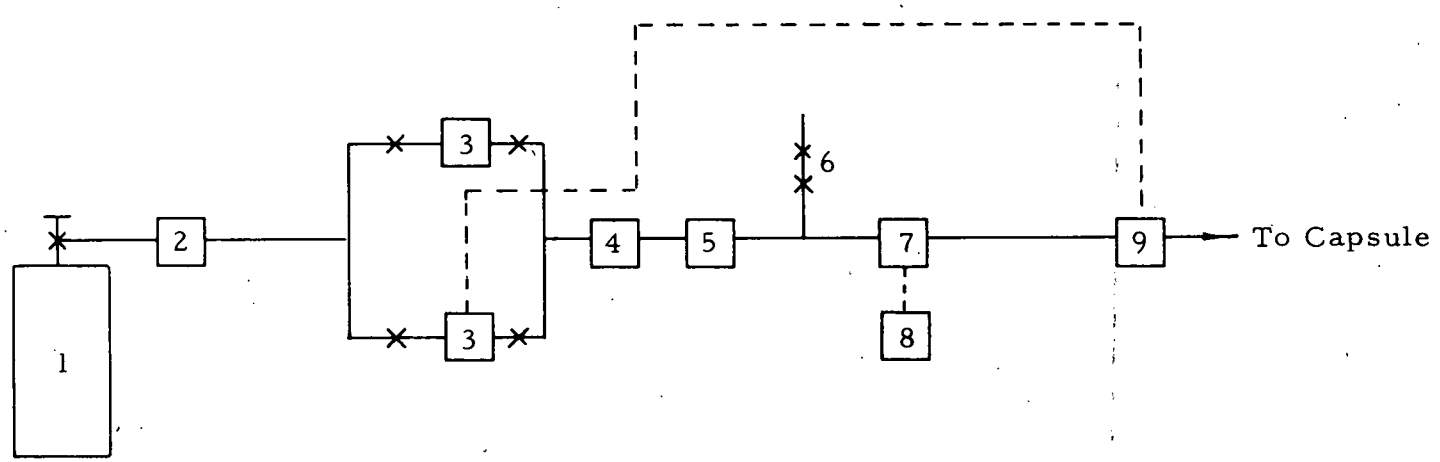

1. Compressed Air Cylinder
2. Pressure Regulator
3. Solenoid Valves
4. Pressure Gauge
5. Flow Controller
6. Bleed Line
7. Pressure Transducer
8. Strip Chart Recorder
9. Inreactor Null Switch

Gas Line
Electrical Line
Valve

7. STATIC GAS RELEASE EXPERIMENT — TASK 07
(W. R. DeBoskey, Task Leader; L. B. Gross)

7.1. Task Objective

The objective of this task is to obtain information on the quantity and species of gases released during irradiation of thoria-urania fuel at varying heat ratings. Heat ratings for these specimens will be essentially identical to those of the thermal conductivity specimens of Task 05 so that some confirmation of thermal conductivity data may be possible providing the operating heat rating of the specimens can be maintained constant during the 60-day irradiation.

7.2. Task Description

The "gas release versus operating heat rating ($\int k d\theta$)" relationship for ThO_2-UO_2 fuel will be developed from postirradiation sampling data. Experiment parameters will be chosen so that the operating heat rating varies up to that required for melting. Some duplication of experiments will be performed for improved statistics. This will be accomplished by loading 5 inreactor capsules with 24 fuel rod specimens as follows:

1. Five specimens of nominal 5 wt% UO_2 in ThO_2, pellets.
2. Six specimens of nominal 10 wt% UO_2 in ThO_2, pellets.
3. Six specimens of nominal 5 wt% UO_2 in ThO_2, vibratory compacted sol-gel powder.
4. Seven specimens of nominal 10 wt% UO_2 in ThO_2, vibratory compacted sol-gel powder.

Properties such as density and isotopic composition of the specimen materials will be determined. Specimen material sources and batches will be the same as those used for Tasks 05 and 06.

Capsules will be irradiated individually for approximately 60 days, during which time a constant neutron flux will be attempted. The inreactor space and capsule equipment console will be shared with Task 05 capsules. Capsule instrumentation will be neutron monitors and thermocouples if practicable.

Postirradiation examination of the 24 specimens will determine the relationship between gas release and heat rating for bulk and powder materials for the two urania compositions investigated. Analysis of characterization and operating data, gas sampling, and radiochemical, isotopic, and ceramographic examinations will be accomplished. All specimens will be examined specifically to corroborate Task 05 data. Samples of these specimens will be made available for postirradiation gas permeability measurements under Task 02.

Gas release data obtained from pellets will be used to establish the general shape and magnitude of the curve representing the relationship between gas release and heat rating. Application of data from sol-gel specimens to this general curve will lead to specific knowledge of the gas release properties of sol-gel fuel.

The design of the capsules for this task will be similar in all respects to the design of the thermal conductivity capsules of Task 05. This reflects the interrelationship of these two tasks. The principal experimental difference, other than the differences in analyses, is the irradiation time. The capsules of Task 05 will be irradiated for only 3 to 4 days—sufficient time for fission products to be generated to permit fuel burnup analysis of meaningful precision. The capsules of this task will be irradiated for approximately 2 months—the time required for sufficient fission gas buildup to allow their analysis with some precision. Although these specimens will be used to corroborate the thermal conductivity specimens, it should be noted that the longer operating time lessens the degree of flux control. From this point of view, the irradiation time of the thermal conductivity experiment should be as short as possible in direct antithesis to the gas release experiment.

7.3. Work Accomplished During This Report Period

Work performed during this initial period included development of the detailed work statement and establishing the capsule design approach.

Since the capsules of this task are similar in all respects to the capsules of the thermal conductivity experiments of Task 05, the design statements made for Task 05 also pertain in this instance. The specimens for this task will be distributed in capsules in accordance with Table 7-1. Their locations are further described in Figures 7-1 through 7-3.

7.4. Planned Work for Next Report Period

In keeping with the plan for the thermal conductivity experiments of Task 05, the design will be formulated and the safeguards report will be written. On obtaining high power BAWTR neutron flux information, fuel enrichments will be determined. Procurement of long-lead-time capsule component materials will commence.

Table 7-1. Capsule Loading Scheme

Capsule number	Specimen number[a]	Specimen type	Specimen position, inches[c]	UO_2 content, wt%	Heat rating, $\int kd\theta$, w/cm	Approximate fuel center temperature, C	Enrichment (fission atom number density)
07-1	1	Pellet[b]	+13, +10	5	49.9	1950	E-1
	2	Powder	+10, + 2	10	80	Melting	E-1
	3	Pellet	+ 2, - 1	5	106	Melting	E-1
	4	Pellet	- 1, - 4	10	78	Melting	E-2
	5	Pellet	- 4, - 7	10	72.5	3150	E-2
	6	Powder	- 7, -15	5	45	2850	E-2
07-2	1	Pellet[b]	+13, +10	10	49.9	1950	E-1
	2	Powder	+10, + 2	5	80	Melting	E-1
	3	Pellet	+ 2, - 1	10	106	Melting	E-1
	4	Pellet	- 1, - 4	5	78	Melting	E-2
	5	Pellet	- 4, - 7	5	72.5	3150	E-2
	6	Powder	- 7, -15	10	45	2850	E-2
07-3	1	Pellet	+12, + 9	10	58.5	2650	E-1
	2	Powder	+ 9, + 1	10	55	3200	E-3
	3	Powder	+ 1, - 7	5	58	Melting	E-3
	4	Powder	- 7, -15	5	25	1850	E-4
07-4	1	Pellet	+12, + 9	5	58.5	2650	E-1
	2	Powder	+ 9, + 1	5	55	3200	E-3
	3	Powder	+ 1, - 7	10	58	Melting	E-3
	4	Powder	- 7, -15	10	25	1850	E-4
07-5	1	Pellet	+12, + 9	5	42.5	1870	E-2
	2	Powder	+ 9, + 1	5	55	3200	E-3
	3	Powder	+ 1, - 7	10	58	Melting	E-3
	4	Powder	- 7, -15	10	38	2550	E-3

[a] Specimens numbered from top to bottom of capsule.

[b] Thermocouple-instrumented specimen.

[c] Top and bottom positions of specimen relative to BAWTR core midplane.

Figure 7-1. Specimen Positions Within Capsules 07-1 and 07-2

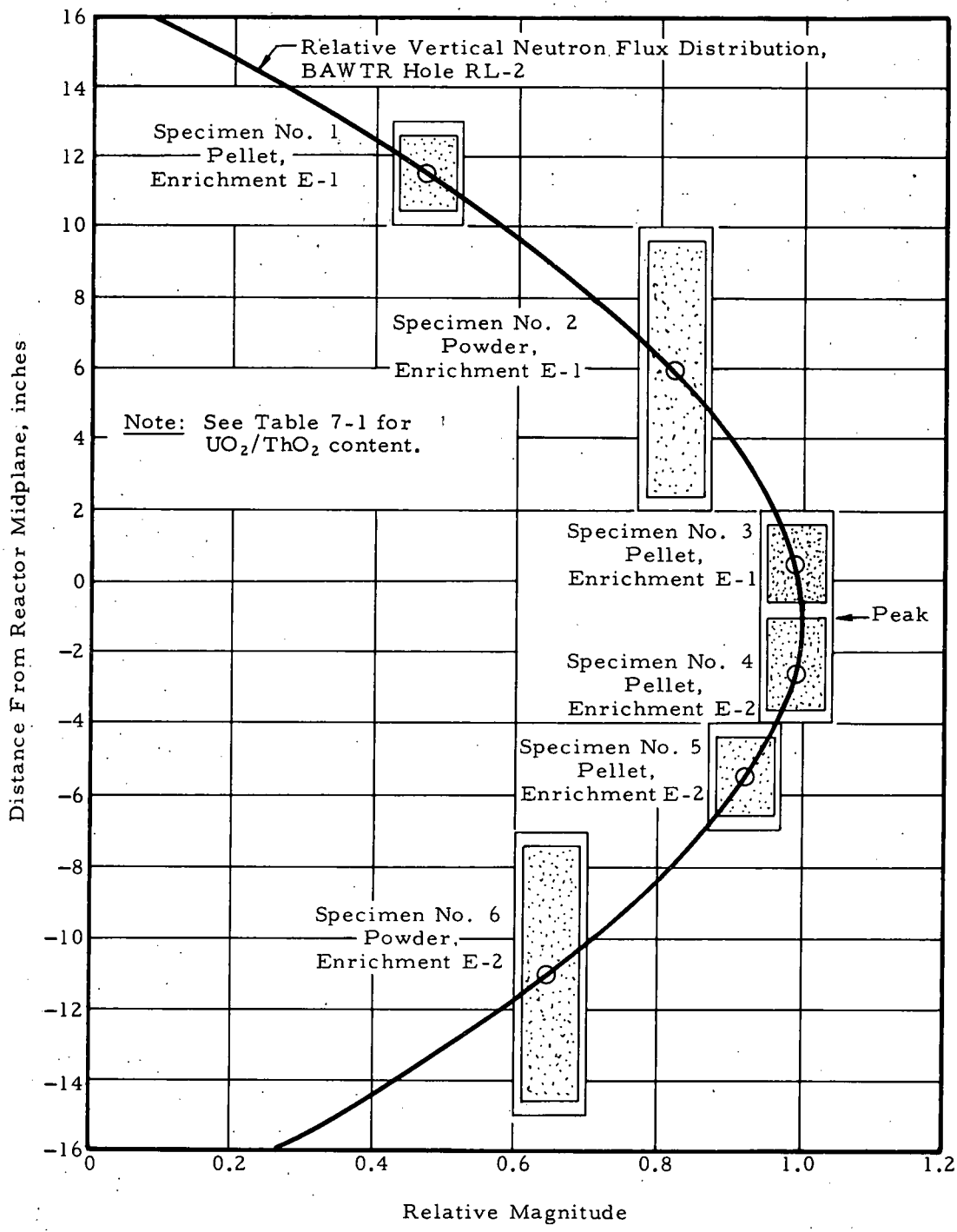

Figure 7-2. Specimen Positions Within Capsules 07-3 and 07-4

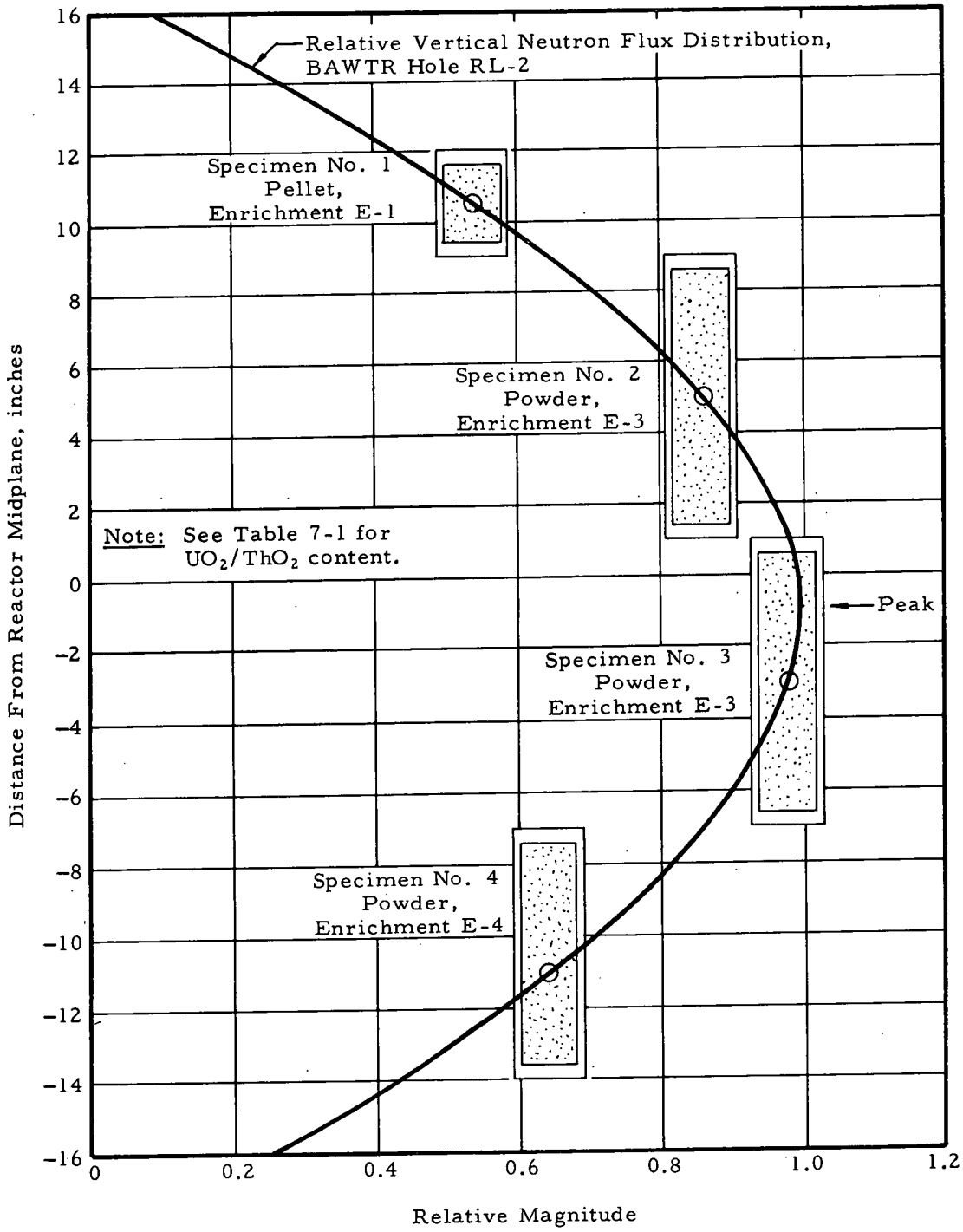

Figure 7-3. Specimen Positions Within Capsule 07-5

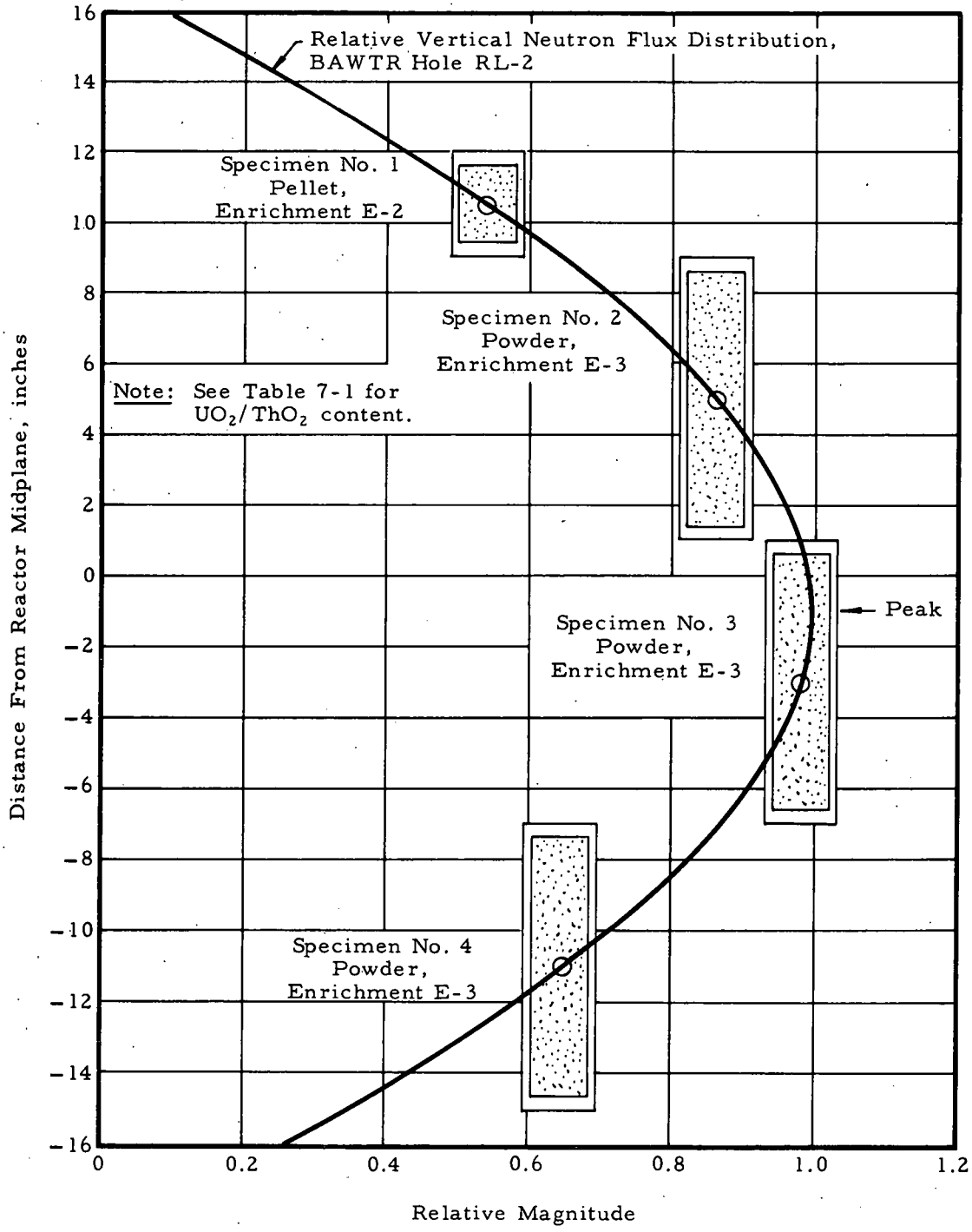

APPENDIX A

Gas Permeability Studies — A Survey
(A. C. Batten)

THIS PAGE
WAS INTENTIONALLY
LEFT BLANK

APPENDIX A

1. Introduction

The objective of Task 59-3096-02 (Gas Permeability of ThO_2-UO_2) is to obtain information concerning the gas permeability characteristics of unirradiated and irradiated specimens of thoria-urania. This information should be useful in the analysis of fission gas movement within fuel rods. During core operation variations in fission gas pressures are likely within the fuel rod, resulting in large variations of driving force for movement of the gas through the structure. Consequently the flow of gas under conditions ranging from low to high pressure differentials should be determined to define probable fission gas movement for all postulated conditions within the fuel rod. The initial program effort is directed toward the design and construction of an apparatus capable of testing the gas permeability of fuel specimens.

Prior to the design and construction of the final experimental apparatus, the program will include preliminary bench-type tests to determine the magnitude of variables involved, as well as establishing preliminary test procedures applicable to the final experiment. To determine definitive experiment requirements, a literature survey of gas permeability technology was made. The purpose of the study was to obtain information on permeability measuring devices, as well as to survey the theoretical gas flow considerations applicable to porous media. Also, a visit was made to the Oak Ridge National Laboratory to see and discuss the gas permeability measuring equipment used by the Analytical Chemistry Division. Results of the literature survey and visit to ORNL are reported herein.

2. Literature Review

2.1. Gas Flow Theory

Permeability is defined as a measure of the capacity of the medium to transmit fluids.[19] Since permeability is determined by measurement of the flow of gas through the porous medium, the basic types of gas flow applicable are briefly reviewed. For a more comprehensive presentation on the flow of gases, refer to Carman[20], Dushman[21], and Barrer[22].

The flow of gas through a circular tube or capillary may be basically defined by the relationship of the size of the tube to the mean free path of the gas molecules. If the radius of the circular tube is large relative to the mean free path of gas molecules flowing through the tube, the type of gas flow will be viscous flow as expressed by Poiseuille's law. This law states that the flow of gas through a circular tube will be directly proportional to the pressure drop per unit length and inversely proportional to the viscosity of the gas. A general form of Poiseuille's law is given by the equation

$$V = \frac{r^2 A \Delta p}{8 \eta L}$$

where

V = volumetric flow rate
r = radius of the tube
A = cross-sectional area normal to flow
Δp = pressure drop
η = viscosity of the gas
L = length along path of flow

The controlling factor for this type of flow is the transfer of momentum between colliding molecules. The velocity of the molecules adjacent to the walls is assumed to be zero, and the viscosity is independent of pressure.

If the mean free path of the gas molecules flowing through a tube is greater than the radius of the tube, viscosity plays no part in the flow since the molecules collide only with the tube walls. This type of flow is called free molecular flow or Knudsen flow.

For an approximation of the type of flow within a tube, the values given for the ratio of the radius r to mean free path λ are:[21, 23]

1. $r/\lambda > 100$ for viscous flow.
2. $r/\lambda < 1$ for Knudsen flow.

Between the viscous flow regime and the Knudsen flow regime is a zone in which both molecular interactions and wall effects must be recognized. Viscous slip and the transition from viscous to Knudsen flow are important in this intermediate zone. A convenient practical technique for treating this zone is to consider all flow to be a linear combination of viscous and Knudsen flows; this technique can be justified on theoretical grounds.[21, 23, 24]

For gas flow through a porous medium, a simple model is chosen where it is commonly assumed that the pore space is equivalent to a bundle of parallel capillaries[20], and the flow of gas is generally defined in terms of both viscous flow and Knudsen flow, which also includes flow in the intermediate zone. This Knudsen-Poiseuille additive relation for gaseous flow is used later to express a permeability coefficient as a result of both viscous flow and Knudsen flow.

2.2. Permeability

Permeability is generally expressed as a coefficient having the dimensions cm^2/sec, which is the same as for a diffusion coefficient.[20] For flow of gas through a porous medium, the definition of permeability coefficient K is[20,25]

$$K = \frac{FL}{\Delta pA}$$

where

F = rate of flow of gas through the specimen in pressure-volume units

L = length of the specimen

Δp = pressure drop across the specimen

A = cross-sectional area of the specimen

The permeability coefficient K depends upon the porous medium and the nature of the gas.[22]

Since a porous body is regarded as being made up of a bundle of parallel capillaries, the permeability coefficient K may be generally expressed in terms of both viscous and Knudsen flows as[20]

$$K = \frac{B_o}{\eta}\bar{p} + \frac{4}{3}K_o\bar{v}$$

where

B_o = viscous flow permeability coefficient

η = viscosity of the gas

$\bar{p}$ = mean pressure of the gas in the porous medium

K_o = Knudsen flow permeability coefficient

$\bar{v}$ = mean thermal molecular velocity

B_o and K_o are specific permeability coefficients and have the dimensions of cm^2 and cm, respectively. Both B_o and K_o are constant characteristics of the porous medium, and once they have been determined

experimentally with one gas, the flow of all other gases through the same medium can be accurately predicted if the viscosities and velocities are known, assuming that the internal structure of the barrier is not altered in any way[26] and that no significant absorption or reaction occurs between the gases and the porous plug.

Another unit for defining permeability is a "darcy", which corresponds to the flow of a single-phase fluid of one centipoise viscosity at a rate of one cubic centimeter per second per square centimeter of cross-sectional area under a pressure of one atmosphere per centimeter.[19] This unit defines a specific permeability and is associated with viscous flow, as generally employed in the petroleum industry[19,20], although several researchers in other fields have reported permeability in darcys[23,27]. In c.g.s. units, one darcy = 9.869×10^{-9} cm^2.

Other units of permeability encountered in the literature are:

cm^4/gm-sec[28]

liter/cm^2-sec[29]

cm^3/sec-cm^2-cm-cm of water[30]

Since permeabilities are reported in many different units, it is important that the reported permeability be precisely defined to be meaningful to others. This may be accomplished by including a nomenclature table in which specific units are given for all the symbols used. This was a common practice observed in the reported literature.[23,31-34]

The expression

$$K = \frac{B_o}{\eta} \bar{p} + \frac{4}{3} K_o \bar{v}$$

is analogous to the linear relationship

$$K = a\bar{p} + b$$

so that a plot of K versus $\bar{p}$ gives an intercept "b" corresponding to the Knudsen term, and the slope "a" equivalent to B_o/η. From the plot, both B_o and K_o may then be determined if the viscosity and molecular velocity are known for the temperature at which the flow measurements were taken. To determine specific permeability coefficients B_o and K_o, which are the desired constants characteristic of the porous medium, flow measurements are taken at several mean pressures in order to

obtain the permeability coefficient K for each of the different mean pressures.

The viscosities for most common gases (including argon, helium, krypton, and xenon) at various temperatures may be obtained from the Handbook of Chemistry and Physics (Chemical Rubber Publishing Co., Cleveland, Ohio). The mean thermal molecular velocity $\bar{v}$ may be determined from the relation

$$\bar{v} = \sqrt{\frac{8RT}{\pi M}}$$

where

R = universal gas constant
T = temperature of the gas
M = molecular weight of the gas

The mathematical derivation for

$$K = \frac{B_o}{\eta}\bar{p} + \frac{4}{3}K_o\bar{v}$$

is given in Reference 24, which also illustrates the procedure described above for the determination of B_o and K_o for several graphite tubes.

2.3. Flow and Pressure Measurements

Flow measurements are generally made by either steady-state or dynamic methods. In the steady-state method, a constant pressure difference is maintained across a specimen while the volumetric flow is measured.[31] Liquid-volume displacement[27,28] and flowmeters, such as the wet-test gas meter[23,35], rotameter[24,33,36], and bubble meter[25] have been used to measure the volumetric flow.

In the dynamic method of flow measurement, the rate of change of pressure within an evacuated vessel is determined. The gas flowing into the vessel of known volume must pass through the specimen. The pressure measurements have been made with a McLeod gauge[25,37,38] or vacuum gauge[29].

In addition to these two methods, some experiments have used specially built-in techniques where the flow of gas is directly related to the flow of mercury in a burette connected to the system[34] or where suction of a gasometer filled with oil is calibrated to relate piston movement to the volume of air pulled through the specimen[30]. Where very low rates

of gas flow were measured, Norton[38] used a mass spectrometer as a recording flowmeter.

The pressure drop across the specimen necessary for calculating permeability (as previously given) is most commonly measured with a manometer.[23,25,28,30,34,35,36] In one reported experiment[24] Bourdon gauges were used, but the American Petroleum Institute does not recommend this type gauge for permeability measurements if reproducible results are desired.[19] For extremely small pressure drops, Malinauskas[25] has used a differential pressure meter which provides absolute pressure readings requiring no corrections for type of gas or barometric pressure.

In addition to the pressure drop across the specimen, other pressure measurements are required to completely define test conditions. These measurements are the inlet and outlet pressures which define the mean pressure in the specimen as

$$\bar{p} = \frac{p_1 + p_2}{2}$$

where p_1 is the inlet pressure and p_2 is the outlet pressure. These measurements have been made with various measuring devices including mercury manometers[24,25,33,37], Bourdon gauges[24,35,37], and vacuum gauges[36]. In steady-state type apparatus, it is common to vent the flow of gas to the atmosphere so that p_2 will always be atmospheric pressure.[24,25,28]

2.4. Effect of Temperature on Permeability

The permeability coefficient K is related to temperature as follows:[20,24]

$$K = \frac{B_o}{\eta}\bar{p} + \frac{4}{3}K_o\sqrt{\frac{8RT}{\pi M}}$$

If B_o and K_o are independent of temperature, the effect of temperature on K may be calculated by applying the appropriate values of viscosity and temperature in the equation. However, any variations of pore structure with changes in temperature would be reflected in changes in the constants B_o and K_o. Such variations can best be determined experimentally since permeability is an extremely sensitive method of detecting changes in pore parameters.[24]

For fine-pore graphite Hutcheon, et al., experimentally found that B_o and K_o were independent of temperature, but the results were restricted to the particular graphite tested.[24] Lack of other reported experiments indicate that gas permeability studies at elevated temperature have been very limited.

2.5. Pore Diameter

The gas flow theory previously presented is restricted to flow through a circular tube. In a porous medium, the pore space is assumed to be equivalent to a bundle of parallel capillaries. Since the actual pore may not necessarily be circular, the size must be expressed in terms of effective diameter of equivalent capillary d_e. For noncircular pipes, the hydraulic radius m is more commonly used where

$$m = \frac{\text{cross-sectional area normal to flow}}{\text{wetted perimeter}}$$

For a circular pipe[20], $m = d_e/4$.

For noncircular capillaries, the permeability coefficient K may be expressed as[20,24]

$$K = \frac{\epsilon m^2 \overline{p}}{k_0 \left(\frac{L_c}{L}\right)^2} + \frac{4}{3} \frac{\delta \epsilon m}{k_1 \left(\frac{L_c}{L}\right)^2}$$

where

ϵ = porosity (the ratio of pore volume to total volume)

m = mean hydraulic radius

k_0 = shape factor for viscous flow in noncircular capillaries

$\left(\frac{L_c}{L}\right)^2$ = tortuosity factor

L_c = length of capillary

L = length of porous medium in direction of flow

δ = dimensionless factor for combining slip flow and Knudsen flow in one term

k_1 = shape factor for Knudsen flow in noncircular capillaries

From this equation, B_o and K_o are then defined as

$$B_o = \frac{\epsilon m^2}{k_0 \left(\frac{L_c}{L}\right)^2}$$

and

$$K_o = \frac{\delta \epsilon m}{k_1 \left(\frac{L_c}{L}\right)^2}$$

so that solution of the equations gives

$$m = \frac{B_o}{K_o} k_0 \frac{\delta}{k_1}$$

Since ϵ, B_o, and K_o are susceptible to direct measurement, and values for k_0 and δ/k_1 have been assigned by Carman[20]. The mean hydraulic radius and tortuosity factor may be determined from permeability measurements. Also, the surface area of a porous medium may be derived from the pore diameter through the relation

$$S_v = \frac{\epsilon}{m}$$

where S_v = surface area per unit volume. To obtain surface area per gram, S_v is divided by the apparent density to give S_o.[24]

Following the foregoing relationships, Hutcheon, et al.,[24] deduced values for mean pore size, surface area, and tortuosity factor for fine-pore graphite. The values of the coefficients led to a mean pore diameter much higher and a surface area much lower than those calculated from adsorption measurements. This was attributed to the presence of porosity which does not take part of the flow, or blind pores. The tortuosity factor appeared to be in keeping with the results of others working on consolidated porous media.

Wiggs[31] approached the relation between gas permeability and pore size differently. For bodies with nonuniform pores, he introduced two mean diameters, one for viscous flow and the other for Knudsen flow. These diameters were calculated by a simple graphical integration of the pore size distribution curve obtained from a mercury porosimeter, using the assumption that gas permeability was analogous to

electrical conductivity. The specific permeability coefficient B_o calculated from porosimeter curves compared favorably with experimental values obtained for three grades of reactor graphite. However, Wiggs considers that there is not sufficient evidence to confirm fully the proposed method of calculating mean diameters, since the exact values of the numerical constants are open to some doubt, namely that the porosimeter indicates the diameter of the largest throat leading into a pore, while the mean hydraulic radius used by Carman is based on an average diameter of the pore.

2.6. Specimen Sealing

To measure precisely the flow of gas across the cross-sectional area of the specimen, sealing of the specimen at the wall of the holder is important to prevent flow of gas between the specimen and the wall. The American Petroleum Institute[19] recommends such sealants as pitch, wax, resin, plastics, and rubber and cautions against using any material that penetrates the pores of the specimen, lest the effective cross-sectional area perpendicular to the path of flow be reduced.

In many of the reported experiments where the porous medium was in the form of a plug, the method of sealing was not mentioned. However, in two references cited, soft rubber and neoprene tubing were used to seal the specimens.[28,34] A unique method for sealing pellets was observed at Oak Ridge National Laboratory, where Wood's metal was used between the pellet and the holder.[25] The expansion of this material upon cooling effected a satisfactory seal, and metallographic examination of the seal showed that Wood's metal did not wet graphite or oxide.

ORNL has measured the gas permeability of some vibratory compacted fuel specimens as part of a program to determine water-logging susceptibility of Kilorod-type fuel rods. ORNL considers that gas does not leak at the tube walls since the small particles effect a satisfactory seal at this location.[39] Surface area measurements are made on all fuel rod specimens to be sure each contains the desired amount of fine particles.

3. Discussion

The survey indicates general acceptance of the gas flow theory involving both viscous and Knudsen flows for determining gas permeability through a porous medium. An expression for the permeability coefficient K in terms of both flows has been derived. From a plot of K vs $\overline{p}$, both B_o and K_o may be determined from the expression

$$K = \frac{B_o}{\eta}\overline{p} + \frac{4}{3}k_o\overline{v}$$

If only Knudsen flow exists, the first term will be zero (no slope), the plot will be a horizontal line, and K will be a constant independent of pressure. If the flow is all viscous flow, the second term will be zero as shown by a zero intercept at zero mean pressure.

It is noted that all the reported experiments have been carried out at mean pressures and pressure drops of a few atmospheres. In the proposed B&W experiment, postulated conditions within the fuel rod make it desirable to also determine gas flow for pressure variations as high as several hundred atmospheres. As the flow rate is increased, viscous flow changes to turbulent flow so that the permeability curve no longer remains linear as described above. However, it cannot be accurately predicted at this time that turbulent flow will be reached at pressure differentials of a few hundred atmospheres using the fuel specimens to be tested. Consequently, the experiment should include flow measurements at both low and high pressure variations in an attempt to establish a relationship between these extreme conditions.

Since most of the reviewed literature concerned the permeability of miscellaneous nonnuclear materials (graphite, refractories, porous glass, porous stainless steel, freeze-dried foods, etc.), reported permeability values are intentionally omitted from this survey. The usefulness of the literature survey findings lies in the theoretical considerations involved and the permeability-measuring devices, which are applicable to almost any porous material.

Elevated temperature studies are considered necessary since data specifically defining the effect of temperature on gas permeability of fuels is lacking. Although Hutcheon[24] found that B_o and K_o were independent of temperature, the assumption that this holds true for nuclear

fuel cannot be made. Any variations in pore structure with changes in temperature would result in changes in B_o and K_o. Also, specimens having the altered fuel structure will contain cracks which are expected to close (and possibly heal) at elevated temperatures, which would affect permeability observed in room temperature experiments. For these reasons, temperature is presently considered a variable in the proposed experiments.

For porous media such as nuclear fuel, the significance of pore diameter as determined by permeability measurements appears to be questionable. Permeability gives a single average value which is represented by the mean hydraulic radius m for uniform pore textures, but is indefinite in other cases.[20] In a fuel specimen, the complex pore space can only be expressed as a distribution of pore sizes. If the pore sizes vary widely, the mean hydraulic radius as determined by permeability measurements must have an insignificant meaning. As a result, if m is obtained by independent measurements from the relation $m = \epsilon / S_v$ and used to calculate B_o, theoretical results will not necessarily agree with experimental values.[20]

Wiggs[31] recognized that the pore diameters in a block of carbon may cover a range of more than 10:1 and therefore introduced mean diameters for each flow term. Although calculated B_o values obtained from an expression using both mean diameters did compare favorably with experimental values, Wiggs expressed some doubt in such comparison on the basis of definition of diameter in each case. It also appears that surface area as determined by permeability measurements may not necessarily agree with independent measurements because of the presence of blind pores, which do not take part in the flow.[24] From these observations it appears that calculated specific permeability coefficients from independent measurements cannot be obtained with any degree of certainty. Therefore, comparison of such values with experimental values will not necessarily confirm the accuracy of the values obtained experimentally.

Although plug-type specimens for room temperature experiments have been successfully sealed using many different materials, a satisfactory sealant for high temperature applications may be difficult to obtain. This is recognized as a potential problem. Some consideration has been given to effecting the seal by thermal expansion of the fuel

pellet; however, this may be successful only at very high temperatures. In vibratory compacted fuel rods, the assumption is made that the fuel powder is tightly compacted against the tube walls to effect a seal.[39] The bench test will be used to determine whether bypassing at the tube walls actually occurs and what influence bypassing has on the test results. If bypassing is excessive, methods of improving the fuel-cladding contact will be evaluated.

Only very limited data concerning gas permeability of nuclear fuel could be found, and these were reported by ORNL.[25,27] Although their fuel specimens were similar to the type to be used in the B&W program, consideration must be given to the relatively different purpose of the ORNL program—that of determining waterlogging susceptibility of Kilorod-type fuel elements. However, maximum use of the reported data will be made wherever it is possible to relate such data to the B&W program. ORNL has indicated an interest and willingness to cooperate in this respect.[25] Figure A-1 is a plot of air permeability data reported by ORNL[27] compared with packed density. Also shown on the same plot are a limited number of argon permeability values. Although the data were generated for direct comparison with water permeability, they could conceivably be used for comparison with B&W results, particularly if air permeability measurements are made on the B&W fuel rod specimens.

In the B&W program, a vacuum gauge will be used to measure low pressures and low flows because vacuum gauges have the advantage of not requiring the usual correction factors associated with mercury gauges (Manometers), and the rate of pressure change may be automatically recorded. Where the rate of flow is extremely low (as predicted for pellet fuel), accurate measurements by any other means are difficult. Further substantiation for using a vacuum gauge may be obtained from results of the bench tests. The Alphatron ionization vacuum gauge having a range of 760 torr to 0.1 micron appears to be suitable as a pressure recorder.[40] Specimen length and conditions for gas flow will be varied to establish suitable test parameters for the final apparatus.

4. Conclusions

1. The flow of gas through a porous medium may involve both viscous and Knudsen types of flow.

2. The permeability coefficient K is experimentally determined by direct measurement of the flow of gas through a porous medium.

3. The permeability coefficient K may be expressed in terms of both viscous and Knudsen flows, from which the specific permeability coefficients B_o and K_o for each flow, respectively, may be determined.

4. The need for gas flow determinations at high pressure variations, where turbulent flow may be encountered, has been established. A relationship between low and high pressure results may then be evaluated.

5. Temperature is presently considered a variable in the proposed experiments.

6. Calculated specific permeability coefficients from independent measurements cannot be used for comparison with experimentally obtained values with any degree of certainty.

7. Sealing of plug-type specimens at elevated temperatures presently poses a potential problem. Also, possible bypassing at the tube walls of vibratory compacted fuel specimens should be evaluated.

8. Gas permeability data for nuclear fuel appears to be very limited.

9. The use of a vacuum gauge for low flow measurements in the proposed experiments appears to have merit.

Figure A-1. Relationship of Permeability to Packed Density (Data From Reference 27)

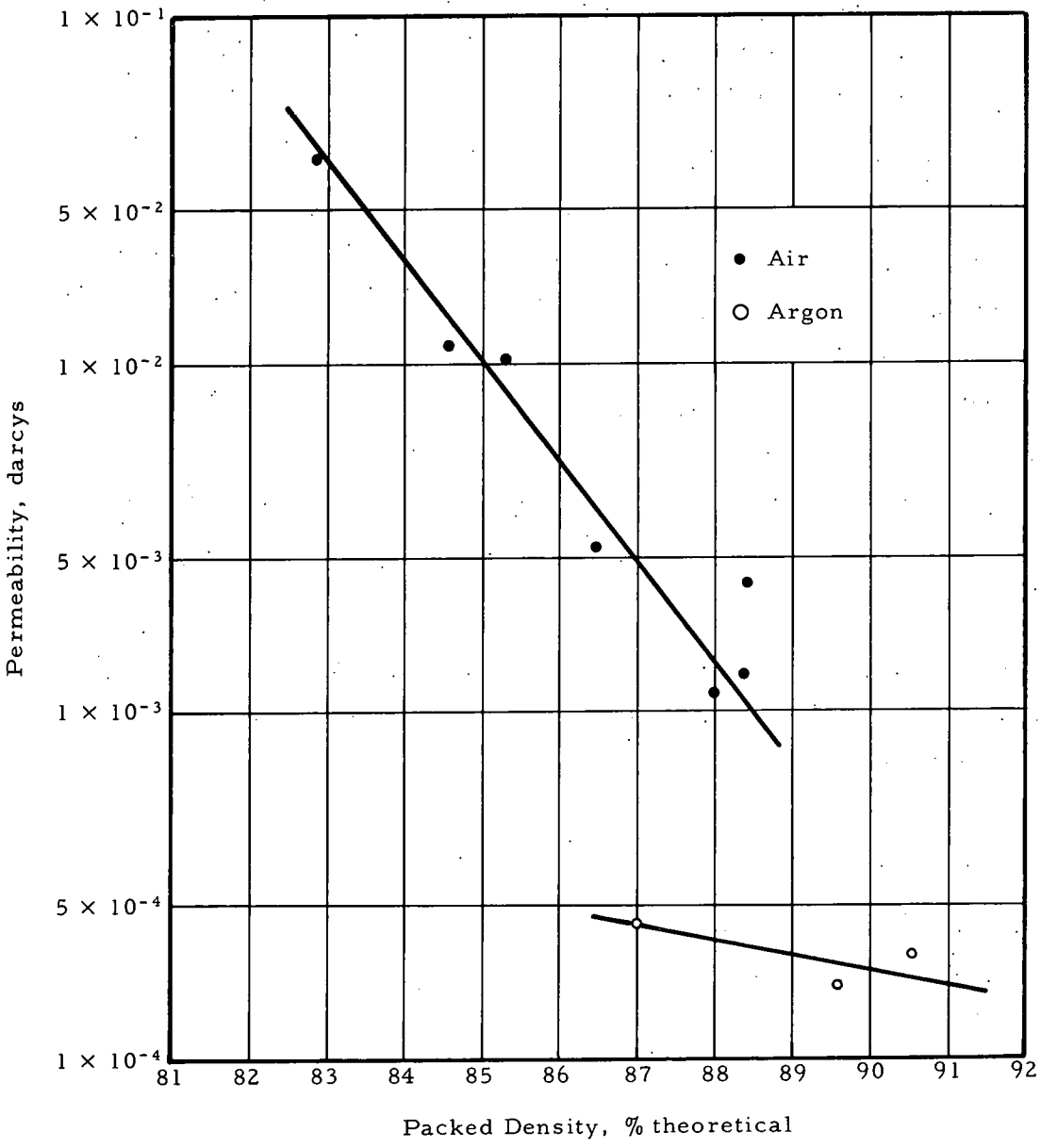

REFERENCES

1 Taylor, R. E., "Analysis for Gases by Vacuum Fusion", Anal. Chem. Acta 21, pp 549-55 (Dec. 1959).

2 Miller, R. I., Analysis for Gases in Uranium, General Electric Company, H. W.-51452, 1962.

3 Champeix, L., "Analysis for H_2 in Uranium by Vacuum Desorption", Mem. Sci. Rev. Met., (July 1960).

4 Methods for Reducing H_2 Content in Uranium, Mallinckrodt Chemical Works, MCW-1412, March 1960.

5 ORNL Progress Report on Thorium Program, ORNL-3385, 1963.

6 Personal Conversation with Dr. O. C. Dean, Group Leader, Chemical Development Section, Chemical Technology Division, ORNL.

7 Lyons, M. F., Coplin, D. H., and Weidenbaum, B., Analysis of UO_2 Grain Growth Data From Out-of-Pile Experiments, GEAP-4411, November 1963.

8 MacEwan, J. R. and Lawson, V. B., "Grain Growth in Sintered Uranium Dioxide: II, Columnar Grain Growth", Journal of the American Ceramic Society 45, 1 (January 1962).

9 DeHalas, D. R. and Horn, G. R., "Evolution of Uranium Dioxide Structure During Irradiation of Fuel Rods", Journal of Nuclear Materials 8, 2 (1963).

10 MacEwan, J. R. and Lawson, V. B., "Grain Growth in Sintered Uranium Dioxide: I, Equiaxed Grain Growth", Journal of the American Ceramic Society 45, 1 (January 1962).

11 Robertson, J. A. L., et al., "Temperature Distribution in UO_2 Fuel Elements", Journal of Nuclear Materials 7, 3 (December 1962).

[12] Hausner, H., Grain Growth of UO_2, Part I, GEAP-4315, August 15, 1963.

[13] Hausner, H., Paper Presented at 66th Annual Meeting of the American Ceramic Society, Chicago, April 18-23, 1964.

[14] Burdg, C. E., The Development and Testing of UO_2 Fuel Systems for Water Reactor Applications - Progress Report Period Ending March 31, 1964, CEND-2863-211.

[15] Treuenfels, E. W., "Emissivity of Isothermal Cavities", Journal of the Optical Society of America 53, 10 (October 1963).

[16] Rasor, N. S. and McClelland, J. D., "Thermal Property Measurements at Very High Temperatures", The Review of Scientific Instruments 31, 6 (June 1960).

[17] Duncan, R. N., Rabbit Capsule Irradiation of UO_2, CVNA-142, June 1962.

[18] Heat Transfer Subcommittee of the Phillips Reactor Safeguard Committee, Calculated Surface Temperatures for Nuclear Systems and Analysis of Their Uncertainties, IDO-16343, June 1957.

[19] Recommended Practice for Determining Permeability of Porous Media, API RP 27, Third Edition, American Petroleum Institute, Division of Production, Dallas, Texas, 1952.

[20] Carman, P. C., Flow of Gases Through Porous Media, Butterworths Scientific Publications, London, 1956.

[21] Dushman, S., Scientific Foundations of Vacuum Technique, Second Edition, John Wiley & Sons, Inc., New York, 1962.

[22] Barrer, R. M., Diffusion In and Through Solids, University Press, Cambridge, 1951.

[23] Wilson, L. H., Sibbitt, W. L., and Jakob, M., "Flow of Gases in Porous Media", Journal of Applied Physics 22, p 1027 (August 1951).

[24] Hutcheon, J. M., Longstaff, B., and Warner, R. K., "The Flow of Gases Through a Fine-Pore Graphite", in Industrial Carbon and Graphite (London Conference, September 24-26, 1957), Society of Chemical Industry, 1958.

[25] Trip Report ACB-23, Trip to Oak Ridge National Laboratory, Oak Ridge, Tenn., July 21, 1964.

[26] Evans, R. B., Malinauskas, A. P., and Truitt, J., Gaseous Transport in Graphite, ORNL-3372, Gas-Cooled Reactor Program, Semi-Annual Progress Report for Period Ending September 30, 1962.

[27] Kelly, M. J. and Griess, J. C., Permeability of Vibratory Compacted Fuels, ORNL-3591, Reactor Chemistry Division, Annual Progress Report for Period Ending January 31, 1964.

[28] Vojnovich, T., McGee, T. D., and Dodd, C. M., Correlation of Slag Resistance With the Pore Structure of an Alumina-Silica Refractory, American Ceramic Society Bulletin, Vol. 43, No. 7, p 514, July 1964.

[29] Lupakov, I. S., Kuz'michev, Y. S., and Zakharow, Y. V., "Determination of the Permeability of Pipe Walls With Respect to Helium", Soviet Atomic Energy (Translated from Russian), Vol. 15, No. 1, p 750, May 1964.

[30] Norton, F. H., Refractories, McGraw-Hill Book Co., Inc., New York, 1949.

[31] Wiggs, P. K. C., "The Relation Between Gas Permeability and Pore Size Distribution in Consolidated Bodies", p 252 in Industrial Carbon and Graphite (London Conference, September 24-26, 1957), Society of Chemical Industry, 1958.

[32] Truitt, J., et al., Transport of Gases Through Ceramic Materials, ORNL-2931, p 149, Oak Ridge National Laboratory, Reactor Chemistry Division, Annual Progress Report for Period Ending January 31, 1960.

[33] Scott, D. S. and Dullien, F. A., "Diffusion of Ideal Gases in Capillaries and Porous Solids", A.I.Ch.E. Journal 8, No. 1, p 113 (March 1962).

[34] Gilliland, E. R., Baddour, R. F., and Russell, J. L., "Rates of Flow Through Microporous Solids", A.I.Ch.E. Journal 4, No. 1, p 90 (March 1958).

[35] Transport of Gases Through Graphite, ORNL-3015, Gas-Cooled Reactor Program, Quarterly Progress Report for Period Ending September 30, 1960.

[36] Harper, J. C., "Transport Properties of Gases in Porous Media at Reduced Pressure with Reference to Freeze-Drying", A.I.Ch.E. Journal 8, No. 3, p 299 (July 1962).

[37] Ward, W. T. and Smith, N. V., Transport of Gases Through Graphite, ORNL-3049, p 297, Oak Ridge National Laboratory, Gas-Cooled Reactor Program, Quarterly Progress Report for Period Ending December 31, 1960.

[38] Norton, F. J., "Helium Diffusion Through Glass", Journal of American Ceramic Society 36, No. 3, p 90 (1953).

[39] Private Communication With Minton J. Kelly, Reactor Chemistry Division, Oak Ridge National Laboratory.

[40] Malinauskas, A. P., "The Role of Absorption in Gaseous Diffusion", M. S. Thesis, Boston College (1958).

[41] Burdg, C. E., The Development and Testing of UO_2 Fuel Systems for Water Applications — Progress Report Period Ending July 31, 1964, CEND-2863-217.

DISTRIBUTION

1. TID-4500, UC-80, 35th Edition (622)

2. United States Atomic Energy Commission, New York Operations Office (4)

   Director, Reactor Development Division (2)
   Reports Librarian (2)

3. United States Atomic Energy Commission, Washington, D. C. (5)

   Hall, EE (2)
   Voigt, WR (3)

4. United States Atomic Energy Commission, Brookhaven Area Office, Upton, Long Island, New York, Attn: Mr. H. Potter

5. Brookhaven National Laboratory, Upton, Long Island, New York, Attn: H. J. C. Kouts

6. Institutt for Atom Energi, Kjeller, Norway

7. The Babcock & Wilcox Company (37)

   Central Files (5)
   DeBoskey, WR
   Deuster, RW (2)
   Edlund, MC
   Gumprich, WC/Mumm, JF
   Halva, CJ
   Harrison, RH/Moore, WT
   Johnson, CR
   Landis, JW
   Library, AED (2)
   Littrell, LW (2)
   Markert, W/Alliance Library
   NDC Files (10)
   Plunkett, DA
   Robinson, GC
   Schomer, RT
   Schutt, PF
   Travis, CC/TRG
   Weissert, LR
   Whitaker, BW
   Williams, DVP